AN ANALYSIS OF SOME DYNAMIC ASPECTS OF TETHERED SATELLITE SYSTEMS

by

ONKAR NATH JHA

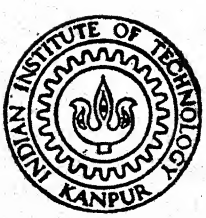

DEPARTMENT OF AEROSPACE ENGINEERING
INDIAN INSTITUTE OF TECHNOLOGY, KANPUR

AUGUST, 1990

AN ANALYSIS OF SOME DYNAMIC ASPECTS OF TETHERED SATELLITE SYSTEMS

A Thesis Submitted
in Partial Fulfilment of the Requirements
for the Degree of
MASTER OF TECHNOLOGY

by

ONKAR NATH JHA

to the

DEPARTMENT OF AEROSPACE ENGINEERING
INDIAN INSTITUTE OF TECHNOLOGY, KANPUR

AUGUST, 1990

AE-1990-M-JHA-ANA

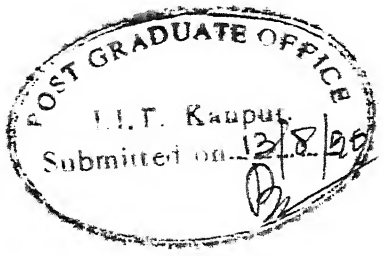

CERTIFICATE

This is to certify that the work **An Analysis of Some Dynamic Problems in Tethered Satellite Systems**, has been carried out under my supervision and has not been submitted elsewhere for a degree.

Krishna Kumar

(Krishna Kumar)
Professor
Aeronautical Engg. Dept.
IIT Kanpur

August, 1990

ACKNOWLEDGEMENTS

I express my grateful thanks to my guide Prof. Krishna Kumar for suggesting the topic, providing the necessary background and his active guidance and encouragement at each stage of this work.

I am also obliged to Prof. A.K. Misra, Dept. of Mechanical Engineering, McGill University, Canada, who during his short visit here at IIT Kanpur was a source of immense help and guidance.

I am grately indebted to my friends and classmates, especially Mr. Sandeep Chojar, Mr. Jatinder Singh and Mr. C.V.K. Singh in helping me with several subtle points of computer programming. I would also like to express my gratitude to Mr. S.R.P. Singh, Mr. D.K. Kaushik and Mr. Rajeeva Kumar, who, as my friends, made my stay here a memorable experience.

Onkar Nath Jha

August, 1990

CONTENTS

LIST OF FIGURES

LIST OF TABLES

NOMENCLATURE

A]	:	Finite element matrix for kinetic energy whose elements involve mass ratios
a_1	:	Semi-major axis of the starting orbit (tether propulsion)
a_2	:	Semi-major axis of the final orbit of a released payload
B]	:	Finite element matrix for rotational energy whose elements involve mass ratios
[C]	:	Transformation matrix in terms of mass ratios
[D]	:	Matrix for the general Eigen Problem
e	:	Eccentricity of the starting orbit (for tether propulsion)
e_2	:	Eccentricity of the final payload orbit
G	:	Universal gravitational constant
H	:	Apogee height of the final payload orbit
H_M	:	Maximum apogee height of the final payload orbit
H_o	:	Initial altitude of the system center of mass
h	:	Angular momentum per unit mass of the system
h_2	:	Angular momentum per unit mass of the payload
$\vec{I},\vec{J},\vec{K}$	:	Unit vectors along inertial co-ordinate axes X,Y,Z.
$\vec{i},\vec{j},\vec{k}$	:	Unit vectors along tether-based co-ordinate axes x,y,z

$\vec{i}_o, \vec{j}_o, \vec{k}_o$: Unit vectors along orbital co-ordinate axes x_o, y_o, z_o

J : Equivalent mass moment of inertia of a two body system; Eq. (2.2.11)

$[K]$: Stiffness matrix

l : Length of the tether in two-body system

l_1, l_2 : Length of the lower and upper tether, respectively in three-body system

l_t : Total length of the tether in three body system

$[M]$: Mass matrix

M : Total mass of the system

M_e : Mass of the Earth

M_i : Mass of the i-th body, i = 1,3

$\bar{m}$: a function of M_1, M_2 and M_3; Eq. (2.2.12)

q_i : i-th generalized co-ordinate

$\vec{R}_2$: Position vector of the payload on its final orbit

R_e : Earth's mean radius

$\vec{R}_i$: Position vector of the i-th body with respect to the center of the Earth

$\vec{R}_o$: Position vector of the system center of mass with respect to the center of the Earth

$\vec{r}_i$: Position vector of the i-th body with respect to the system center of mass

r_l : Length ratio (= l_2/l_1)

r_{31}, r_{32} : Mass ratios equal to M_3/M_1, and M_3/M_2, respectively

T	:	Total kinetic energy of the system
T_{M_i}	:	Kinetic energy associated with the attitude motion of the i-th body, i = 1,3
T_i	:	Tension in the i-th tether
T_{orb}	:	Orbital kinetic energy of the system
T_{nonorb}	:	Kinetic energy associated with the attitude motion of the system.
T_t	:	Resultant tension in the tether (= T_2-T_1)
t	:	Time
V	:	Total potential energy of the system
V_{M_i}	:	Potential energy associated with the attitude motion of the ith body, i = 1,3
V_i	:	Potential energy of the i-th body
V_{orb}	:	Orbital potential energy of the system
V_{nonorb}	:	Potential energy associated with the attitude motion of the system
$\vec{v}_2$	:	Linear velocity of the payload
X,Y,Z	:	Earth centered inertial co-ordinate system
x,y,z	:	Tether-based and orbital co-ordinate for the two-body and three-body tethered systems, respectively
x_o,y_o,z_o	:	Orbital co-ordinate system for the two-body system
y_t	:	Spatial variable measured from mass M_1
α	:	Pitch rotation
α_i	:	Pitch angle of the i-th tether, i = 1,2

α_r : value of the pitch angle at the time of release

α_o : Initial pitch amplitude

$\alpha_i(0)$: Initial pitch amplitude of oscillation of the i-th tether, i = 1,2

β : Angle between linear velocity and position vector of the payload

δ : Tolerance on the error

ϵ : Total energy per unit mass of payload

θ : True-anomaly

θ_r : Optimum position of the system center of mass on the starting orbit at the time of release

Λ : Lagrangian multiplier

λ : Eigenvalue related to frequency as $\lambda = i\omega$

μ : Universal gravitational constant times mass of the Earth

μ_i : Mass ratio equal to M_i/M, i = 1,3

ρ_t : Mass per unit length of the tether

Ω : Mean orbital rate

$\bar{\omega}$: Angular velocity of tether-based co-ordinate system

ω : Frequency of oscillation

ω_1, ω_2 : frequencies of oscillation of the three-body tethered system

dot : Derivative with respect to time

prime : Derivative with respect to the true-anomaly or non-dimensional time τ

ABSTRACT

In this thesis, two important dynamic aspects of tethered satellite system are investigated. In the first part, attention is focussed on payload raising potential of dumb-bell tethered satellite configuration executing pitching libration in circular as well as elliptic orbits. The effect of librations on the maximized gain in orbit size subsequent to tether cut-off at optimal location is examined. The study clearly demonstrates the usefulness of having the dumb-bell tethered system in highly elliptic orbit for substantially enhancing the tether's payload raising capability. In some extreme cases, e.g. with e = 0.5, the increase in the payload major axis can go up to as high as ~ 50 times the length of the tether, much more than the corresponding figure reported in the recent literature.

In the next and final phase, the in-plane transverse vibrations of the two tethers connecting the three-body constellation in its stable equilibrium configuration are investigated. The natural frequencies of vibration in the first few important modes are obtained using finite element approach. The results obtained here may be of considerable general importance for a preliminary design of various components or subsystems in the tethered constellation. Besides, the analysis presented may be found useful for extracting information on tension in the vibrating tethers connecting the satellite constellation.

CHAPTER I

INTRODUCTION

1.1 PRELIMINARY REMARKS

Advent of the space shuttle and the space station have presented a wide range of possibilities for space exploration and exploitation. One approach to this end is the concept of Tethered Satellite System (TSS). However, the idea is not new. Indeed in 1895, Tsiolkovsky suggested linking large masses by a long thin string to exploit weak gravity gradient forces [1].

The possibility of using tethers in space has generated considerable interest. Tethered Satellite Systems are general candidates for enhancing future shuttle capabilities. They allow the deployment and retrieval of payloads down to orbits which cannot otherwise be considered due to high drag decay.

Operations with tethered vehicles were successfully carried out during two Gemini missions[2] using a short tether. The manned spaced vehicles Gemini XI and Gemini XII were tethered to unmanned Agena vehicles. The former used a rotating configuration that was maintained by the Gemini thruster reaction control system, whereas Gemini XII flight test demonstrated a gravity gradient specialized configuration.

This very year i.e., in 1990, it was proposed to fly the first tether deployer/retrieval system in space. This mission, delayed due to temporary setback to the shuttle programme

following the challenger disaster, was to fly the Tethered Satellite System[3,4] developed and funded by NASA and the Italian National Space Plan (CNR). The first mission is to deploy a 500 kg subsatellite upward from the shuttle on a 2 mm thick Kevlar tether 20 km long, where the gravity gradient forces will stabilize the two masses along a vertical configuration. It is proposed to investigate the interaction of the tether, having a conducting core, with Earth's magnetic and ionospheric environment. A second mission is to be flown about two years later, using the same deployer system, to tether a subsatellite 100 km downward (the shuttle will be at 220 km altitude) to investigate Earth's upper atmosphere. Several other tether or tether related missions are in the planning and development stage. The 1990's should see at least half a dozen such missions which will demonstrate specific tether capabilities and increase our understanding of their benefits and behaviour in space[5].

Several possible applications of TSS have been proposed for a multitude of uses. A few of them are summarized below:

(1) Low altitude scientific experiments: A subsatellite may be deployed into the upper atmosphere from the shuttle to provide scientists with a means of measurements of the physical properties of atmosphere. It would also permit long term observations of various phenomena in the lower thermosphere.

(2) Deployment of payloads into new orbits or retrieval of satellites for servicing.

(3) Antenna for radio astronomy and low frequency communications.

(4) Power Generator: A long insulated conducting tether moving at a high speed cutting Earth's magnetic lines of force induces e.m.f. Such a system could be used as an emergency power generator.

(5) Micro gravity experiments: A tether connected system aligned with the local vertical can produce an artificial gravity for both the end bodies. The tension in the tether caused by the gravity gradient pulls these bodies towards their system centre of mass (CM). The weak gravity level thus produced (0.01 to 0.1g) makes this system ideal for low gravity experiments.

(6) Transportation and Space Constellation: A tether can be used for cargo transfers or deposition of hazardous facilities to a safe distance or even for capturing an artificial comet.

Besides, there are many other possible applications proposed but not discussed here for the sake of brevity.

The conceptual use of tether in affecting an overall propulsion economy for "enlarging" a payload orbit is now well established. This is accomplished by launching the space transportation system along with its tethered but undeployed subsatellite into an orbit. The subsequent deployment of small payload through tether followed by its release raises the small payload orbit while the shuttle deploying it gets correspondingly lowered in this "momentum exchange" manoeuvre. In recent years, several investigators have shown that release and capture of payloads through tethers are practical and fully stable operations. The underlying concept is as follows: the subsatellite when held by a tether deployed upwards has the same angular velocity as the main orbiter, which implies a subsatellite

velocity greater than that needed for the orbit at its altitude. Thus if now released by cutting the tether, it will lie on an elliptic orbit around the Earth having a greater semi-major axis than that of the tethered two body system. More explicitly, the three steps involved in this operation are as follows:

(i) Deployment of the payload to a planned release altitude using tether.

(ii) Disconnection of the payload from the tether enabling it to rise it to a higher orbit.

(iii) Reeling back the tether into the shuttle, an operation called retrieval.

First part of the thesis deals with this application.

Dynamics of the tethered system is rather complicated. It involves three important aspects of motion. The orbital motion refers to the translational motion of the CM of the tethered satellite system while the attitude dynamics is concerned with the "rigid body" angular motion of the system about the CM. Unlike the rigid body system, here we also have a flexible tether which is responsible for sharing the energy in its longitudinal as well as transverse modes of vibrations. For complete understanding of the system dynamic behaviour, in general, all the three aspects must be examined simultaneously. This problem gets further complicated by the presence of environmental disturbing effects such as atmospheric drag, asphericity of the Earth, Earth's magnetic field, gravitational pull of other celestial bodies, etc.

The dynamics of tethered satellite systems has received a great deal of attention during the last decade and at present fairly complete dynamical models are available. But with a few

exceptions, most investigations usually deal with the rotational motion of the tether. However, of the various aspects of motion of the tethered satellite systems, the associated elastic oscillations of the tether have received relatively little attention. Later part of the work is devoted to the transverse vibrations of the tether in the three body system connected by a pair of tethers.

1.2 A BRIEF REVIEW OF THE LITERATURE

A fairly large number of models used by various investigators in an attempt to obtain some insight into the complex dynamics of the system have been summarized by Mishra and Modi[6,7]. Here, we present literature review separately for the two topics: release of the payload of a two body system and the transverse vibrations of the three body tethered constellations.

1.2.1 Release of Payloads

The general concept of releasing a tethered payload from a shuttle is shown in Fig. 1. When deployed upwards the payload travels faster than the circular orbit speed required at its altitude. On the other hand the shuttle possesses a speed lower than what is needed to sustain its orbit at this altitude without the tether. If the tether is now severed, the payload would be in a transfer orbit to a higher apogee while the shuttle would drift to a lower perigee.

Von Tiesenhausen[8] reported that in order to have the released payload ending up in a circular orbit, the initial shuttle orbit needs to be elliptical.

Bekey[9] reported that for a two body tethered system in a

circular orbit the released payload would follow a different path with its perigee at its release point and the apogee on the diametrically opposite side of the Earth. If the release occurs while the payload is librationally stable and along the local vertical, the altitude of the apogee would be higher than the perigee ~ seven times the length of the tether. A suitably pitching payload can rise to much higher with the corresponding gain now going up to fifteen times the length of the tether.

Zine Eddine Amier[10] considered a maximization procedure to determine the optimum time of release of the payload so that the altitude gain for the two body system in a circular orbit on tether cut-off is maximized. He concludes that the gain in apogee altitude for the librating tethered satellite system can be up to even as high as sixteen times the tether-length.

1.2.2 Space Constellations

Until recently, the interest of the investigators in tethered system applications was focussed on two body tethered systems. There are, however, interesting situations involving three orbiting bodies connected by tether(s), such as the space station based tethered constellations and transportation of a cargo from one end body to the other. A space constellation is defined as a fixed arrangement of three or more masses connected by tethers.

Since the concept is relatively new, there are few dynamical studies in this area. The first dynamical formulation of a three body tethered system was attempted by Liu[11]. He considered the attitude dynamics in the orbital plane during the mass transport from one end body to the other. His formulation led to six non-linear ordinary differential equations in the six variables.

Since there can be only three independent generalized coordinates in this case, three constraints were also obtained. In an alternate formulation, he utilized four generalized coordinates with just one constraint. Unfortunately, in either case the author found it difficult to solve, even numerically, the complicated system of equations subjected to the algebraic constraints.

A more efficient formulation for the three body tethered systems was presented by Lorenzini et.al.[12] Neglecting the mass of the tethers the frequency of oscillation of the line joining the end bodies with respect to the system centre of mass was found to be approximately $\omega = (\sqrt{3/R_2} - 1)\,\Omega$, where R_2 is the ratio of mass of the middle body to the total mass and Ω is the overall system orbital frequency.

Zine-Eddine Amier[10] has derived the equations governing the two-dimensional dynamics of three body tethered constellations in an Earth Orbit. He has also determined the equilibrium configurations and stability of motion around the equilibrium configurations.

1.3 PURPOSE AND SCOPE OF THE INVESTIGATION

From the literature review, it is clear that the attitude dynamics, i.e. the swing motion, can play a major role in the release of payload and significantly alter the orbital motion of the released payload. On the other hand, the dynamical analysis, especially the vibrations of the tethers connecting three body constellation is at its infancy. Here, we consider these two topics as our main objective for the investigation. First, the effects of the various parameters of the two body tethered system

on the maximum gain in the major axis of the payload, starting from an elliptical orbit, are examined. Next undertaken is an analysis of the transverse tether vibrations of three body constellations in a vertical stable configuration.

CHAPTER II

TWO-BODY TETHER SYSTEM

2.1 INTRODUCTION

A subsatellite deployed from an artificial earth satellite, and attached by a tether constitutes a two-body tether system. During deployment or retrieval, the system centre of mass continues to move along a Keplerian orbit. In general, the dynamic study covering various aspects of motion is fairly involved. However, several of these can be investigated with sufficient accuracy by simplified tether models. In our formulation, the mass of the tether is taken into account while obtaining the total kinetic and potential energies of the tethered system. The kinetic energy is calculated as a sum of that associated with a translational motion as well as that for the relative altitude motion about the mass centre. Thus the dynamics is separated in the orbital motion of the centre of mass and the relative motion of end masses with respect to the local frame connected to the centre of mass (attitude motion). No restrictions on length of the tether or on mass ratio of the end-masses are imposed.

The system equations of motion are developed using Lagrangian formulation assuming the external forces to be only gravitational. The equations are solved with a view to study the variation of the total energy of the subsatellite as the two-body tether system orbits around the earth. This enables us to identify the instant at which the total energy of the subsatellite is a maximum. It is at this point when cutting-of-the tether maximizes the momentum transfer from the shuttle to the subsatellite. Subsequent growth in the satellite orbit is assessed in terms of the net increase in the semi-major axis of the payload achieved over that of the tethered system. For simplicity, we only consider the pitching librations. The out-of-plane librations and tether vibrations are ignored.

2.1.1 Approach to the Problem

To find out the optimum time of release to maximize the "altitude gain", various methods are available in the literature. A few of them are: (1) Maximizing velocity of the subsatellite at the time of cutting the tether, (2) Finding pitch angle (α) and its derivative at every position along orbit and making simultaneously α to be maximum and α' to be zero at the point of cutting the tether. All these methods seem to work fine as long as initial orbit of the system c.m. is circular. For elliptic orbits, since system equations of motion are non-linear differential equations, these methods tend to diverge as eccentricity of the orbit increases.

In the present investigation, a new approach has been followed. Instead of trying to maximize velocity or pitch angle

(α) at the time of cutting, what has been tried is to maximize the total energy. As is known, the total energy per unit mass for the subsatellite is

$$\epsilon = -\mu/2a,$$

where,

μ is Earth's gravitational constant

a is semi-major axis

The orbit apogee, can be calculated from the instantaneous position and velocity vectors of the subsatellite at the cut-off point. The position and velocity vectors become known once we solve the system equations of motion. These equations are non-linear and non-autonomous. An approximate analytical as well as an "exact" numerical solution has been attempted.

The approach followed here turns out to be a simple and elegant one. It works for both circular and elliptic starting orbits and no divergence has been observed.

2.2 DEVELOPMENT OF THE SYSTEM EQUATIONS OF MOTION

2.2.1 Description of the System

The system under consideration is shown in Fig. 2. Masses M_1 and M_2 represent the orbiter (shuttle or space station) and the payload (satellite) respectively. The long tether joining M_1 and M_2 has a mass ρ_t per unit length and length l_t. The instantaneous centre of mass (CM) of the system is located at a radial distance R_o along the local vertical from the centre of the Earth and its true-anomaly is θ. We consider three sets of coordinate axes. The global coordinate system, XYZ, is an inertial reference frame fixed at the centre of the Earth. The other two coordinate

systems, xyz and $x_o y_o z_o$ are rotating frames having their origin at the system centre of mass (CM). In $x_o y_o z_o$ coordinate system, z_o axis is along the local horizontal, y_o-axis is along the local vertical and x_o-axis is normal to the orbital plane. In xyz coordinate system, however, y-axis lies along the tether line, z-axis is normal to y-axis and in the orbital plane while x-axis is normal to the orbital plane. We limit ourselves to only in-plane librations. Thus the orientation of the tethered system relative to $x_o y_o z_o$ frame is described by pitch angle α only. The pitch angle α is the satellite rotation about orbit normal x_o-axis. The unit vectors along the three set of axes are respectively $\hat{I}$, $\hat{J}$, $\hat{K}$; $\hat{i}_o$, $\hat{j}_o$, $\hat{k}_o$ and $\hat{i}$, $\hat{j}$, $\hat{k}$. The radius vectors $\vec{r}_1$ and $\vec{r}_2$ denote the position vectors of masses M_1 and M_2 from the CM of the system. The position vector of any arbitrary point on tether, with respect to the CM, is denoted by $\vec{r}_3$ and can be determined uniquely in terms of $\vec{r}_1$ and $\vec{r}_2$.

Orbital dynamics and attitude dynamics have been considered separately assuming the perturbation of the orbital motion due to attitude motion to be negligible[12]. However, the attitude motion of the entire system may have non-negligible influence on the orbit of the payload after release. The other assumptions are:

(i) Rigid tether, ignoring its vibrations - this part is separately considered for space constellations in Chapter III.

(ii) The orbiter and payload regarded as point-masses.

(iii) Only external force acting on the system being the Earth's gravitational force, the other forces like atmospheric

drag, effect of Earth's electromagnetic field, solar radiation pressure, gravity forces due to other space bodies etc. are ignored.

These assumptions considerably simplify the mathematical model, but the analysis is primarily directed to bring out the basic features so essential to study an advance model.

2.2.2 Kinematics of the System

Referring to Fig. 2, since CM is the centre of mass, we have the following relation,

$$M_1 \vec{r}_1 + M_2 \vec{r}_2 + \int_{M_3} \vec{r}_3 \, dm = 0 \qquad (2.2.1)$$

And, from geometric considerations,

$$\vec{r}_2 - \vec{r}_1 = \vec{l}_t \qquad (2.2.2)$$

where $|\vec{l}_t|$ is l_t, the length of tether.

If we resolve the vectors in their components along the x, y, z axes introducing a spatial variable y_t measured along the tetherline from the mass M_1, it allows us to write

$$\vec{r}_3 = (y_t - r_1)\,\hat{j}$$

$$\vec{r}_2 = r_2\,\hat{j}$$

$$\vec{r}_1 = -r_1\,\hat{j}$$

Substituting these into (2.2.1), we have

$$\left[-(M_1 + M_2)\, r_1 + M_2\, l_t + \rho_t \int_0^{l_t} (y_t - r_1)\, dy_t \right] \hat{j} = 0$$

which yields the following equation

$$-(M_1 + M_2 + M_3)\, r_1 + (M_2 + \tfrac{1}{2} M_3)\, l_t = 0$$

i.e.
$$r_1 = \frac{M_2 + \frac{1}{2} M_3}{M}\, l_t \qquad (2.2.3)$$

where, M_3 denotes the mass of the tether.

Similarly,

$$r_2 = \frac{M_1 + \frac{1}{2} M_3}{M}\, l_t \qquad (2.2.4)$$

where, the total system mass $M = M_1 + M_2 + M_3$.

2.2.3 Kinetic and Potential Energies

The total kinetic energy and the total potential energy, each can be separated into two parts, one for the orbital motion and the other for the attitude motion. For example,

$$T = T_{orb} + T_{nonorb}$$
$$V = V_{orb} + V_{nonorb}$$

We will consider each part separately. For the orbital motion, using polar coordinates R_o and θ for the CM, we have

$$T_{orb} = \frac{1}{2} M \left[\dot{R}_o^{\,2} + R_o \dot{\theta}^2 \right] \qquad (2.2.5)$$

and
$$V_{orb} = -\mu \frac{M}{R_o} \qquad (2.2.6)$$

For non-orbital part, we first obtain the energy expressions relative to the xyz coordinate system and then use the following transformations

$$\begin{Bmatrix} \hat{i}_o \\ \hat{j}_o \\ \hat{k}_o \end{Bmatrix} = \begin{bmatrix} 1 & 0 & 0 \\ 0 & \cos\alpha & -\sin\alpha \\ 0 & \sin\alpha & \cos\alpha \end{bmatrix} \begin{Bmatrix} \hat{i} \\ \hat{j} \\ \hat{k} \end{Bmatrix} \qquad (2.2.7)$$

$$\begin{Bmatrix} \hat{I} \\ \hat{J} \\ \hat{K} \end{Bmatrix} = \begin{bmatrix} 1 & 0 & 0 \\ 0 & \cos\theta & -\sin\theta \\ 0 & \sin\theta & \cos\theta \end{bmatrix} \begin{Bmatrix} \hat{i}_o \\ \hat{j}_o \\ \hat{k}_o \end{Bmatrix} \qquad (2.2.8)$$

Also, noting that $\bar{\omega}$, the angular velocity of xyz frame has the following components

$$\omega_x = (\dot{\theta} + \dot{\alpha}); \quad \omega_y = \omega_z = 0$$

so that

$$\dot{\vec{r}}_1 = \vec{\omega} \times \vec{r}_1, \quad \dot{\vec{r}}_2 = \vec{\omega} \times \vec{r}_2, \quad \dot{\vec{r}}_3 = \vec{\omega} \times \vec{r}_3,$$

Using these relations to transform the energy expressions, after going through fairly straightforward but lengthy algebraic manipulations, one can show that

$$T_{nonorb} = \frac{1}{2} J (\dot{\theta} + \dot{\alpha})^2 \qquad (2.2.9)$$

$$V_{nonorb} = \frac{1}{2} \frac{\mu J}{R_o^3} [1 - 3\cos^2\alpha] \qquad (2.2.10)$$

where J represents the moment of inertia of the system around an axis passing through CM and perpendicular to the tether and can be expressed as

$$J = \bar{m} l_t^2 \qquad (2.2.11)$$

where,

$$\bar{m} = M_1 \left(\frac{M_2 + \frac{1}{2} M_3}{M} \right)^2 + M_2 \left(\frac{M_1 + \frac{1}{2} M_3}{M} \right)^2$$

$$+ M_3 \left\{ \frac{1}{3} - \frac{M_2 + \frac{1}{2} M_3}{M} + \left(\frac{M_1 + \frac{1}{2} M_3}{M} \right)^2 \right\}$$

In the special case, if one considers M_1 to be very large compared to M_2 and M_3, $\bar{m}$ reduces to

$$\bar{m} = M_2 + \frac{1}{2} M_3 \qquad (2.2.12)$$

2.2.4 Equations of Motion Before Release

The equations (2.2.5), (2.2.6) and (2.2.9), (2.2.10) give the expressions for the total kinetic energy and potential energy. Using the lagrangian formulation, one can show that the equation governing the pitch oscillations is[7]:

$$\alpha'' - \left(\frac{2e \sin \theta}{1+e \cos \theta} \right) (\alpha' + 1) + \frac{3}{1 + e \cos \theta} \cos \alpha \sin \alpha = 0 \qquad (2.2.13)$$

2.3 ORBITAL MOTION AFTER RELEASE

In the previous section equations of motion were developed for the tether system before release considering both orbital and attitude dynamics. However, after the release of the tether we have two unconnected point masses, so we need to consider simply the orbital dynamics for each of the two separated masses. Since our interest lies in the motion of subsatellite, let us denote its final orbit apogee and eccentricity by a_2 and e_2 respectively. To calculate these we need to know its position and velocity vectors, $\vec{R}_2$ and $\vec{V}_2$ respectively, at the time of release.

2.3.1 Position and Velocity Vectors Just Before Release

From Fig. 2, we have the vector relation

$$\vec{R}_2 = \vec{R}_o + \vec{r}_2 \qquad (2.3.1)$$

where,

$$\vec{r}_2 = r_2 \hat{j} \qquad (2.3.2)$$

and the distance r_2 is a function of masses M_1, M_2 and M_3 as given by Eq. (2.2.4), while R_o is obtained from the initial orbit parameters a_o and e_o using the following well known relation for ellipse in polar coordinates (R_o, θ).

$$1/R_o = 1 + e \cos \theta \qquad (2.3.3)$$

where the semi-latus rectum, l, is given by

$$l = a (1 - e^2) \qquad (2.3.4)$$

Therefore, if θ be the true anomaly at the point of release in the original orbit, we have

$$R_o = \frac{a_o (1 - e_o^2)}{1 + e_o \cos \theta} \qquad (2.3.5)$$

Also, for the central force motion

$$R_o^2 \dot{\theta} = \text{const.} = h \qquad (2.3.6)$$

where, h is specific angular momentum and is given by,

$$h^2 = \mu \cdot l; \qquad (2.3.7)$$

These led to the final results as given below:

$$\dot{\theta} = \frac{h}{R_o^2} \qquad (2.3.8)$$

$$\dot{R}_o = \frac{\mu}{h} (e_o \sin \theta) \qquad (2.3.9)$$

$$\ddot{\theta} = \frac{-2\dot{R}_o \dot{\theta}}{R_o} \tag{2.3.10}$$

$$\ddot{R}_o = \frac{h^2}{R_o^3} - \frac{\mu}{R_o^2} \tag{2.3.11}$$

Also, the orbital angular velocity, Ω, is given by

$$\Omega = \sqrt{\mu/a^3} \tag{2.3.12}$$

Now, we can write Eq. (2.3.2) in terms of global unit vectors $\hat{I}$, $\hat{J}$, $\hat{K}$ as:

$$\vec{r}_2 = [T_\theta]\,[T_\alpha] \begin{Bmatrix} 0 \\ r_2 \\ 0 \end{Bmatrix} \tag{2.3.13}$$

where $[T_\theta]$ and $[T_\alpha]$ are transformation matrices given by Eqs. (2.2.7) and (2.2.8). Also,

$$\vec{R}_o = R_o \cos\theta\, \hat{J} + R_o \sin\theta\, \hat{K} \tag{2.3.14}$$

So, Eq. (2.3.1) becomes,

$$\vec{R}_2 = [R_o \cos\theta + r_2 \cos(\theta + \alpha)]\, \hat{J} + [R_o \sin\theta + r_2 \sin(\theta + \alpha)]\, \hat{K} \tag{2.3.15}$$

where α is the pitch angle shown in Fig. 2.

The position vector being thus known, it is easy to calculate the velocity vector $\vec{V}_2$. For, differentiating Eq. (2.3.1) yields

$$\vec{V}_2 = d\vec{R}_2/dt + d\vec{r}_2/dt = d\vec{R}_2/dt + \vec{\omega} \times \vec{r}_2 \tag{2.3.16}$$

where,

$$\frac{d\vec{r}_2}{dt} = \begin{vmatrix} \hat{I} & \hat{J} & \hat{K} \\ \dot{\theta} + \dot{\alpha} & 0 & 0 \\ 0 & r_2 \cos(\theta+\alpha) & r_2 \sin(\theta+\alpha) \end{vmatrix}$$

$$= -[r_2 (\dot{\theta}+\dot{\alpha}) \sin(\theta+\alpha)]\,\hat{J} + [r_2 (\dot{\theta}+\dot{\alpha}) \cos(\theta+\alpha)]\,\hat{K} \qquad (2.3.17)$$

And differentiating Eq. (2.3.14),

$$d\vec{R}_o/dt = [\dot{R}_o \cos\theta - R_o \dot{\theta} \sin\theta]\,\hat{J} + [\dot{R}_o \sin\theta - R_o \dot{\theta} \cos\theta]\,\hat{K} \qquad (2.3.18)$$

Therefore,

$$\vec{V}_2 = [\dot{R}_o \cos\theta - R_o \dot{\theta} \sin\theta - r_2 (\dot{\theta}+\dot{\alpha}) \sin(\theta+\alpha)]\,\hat{J} + [\dot{R}_o \sin\theta - R_o \dot{\theta} \cos\theta + r_2 (\dot{\theta}+\dot{\alpha}) \cos(\theta+\alpha)]\,\hat{K} \qquad (2.3.19)$$

The magnitudes of the position and velocity vectors, R_2 and V_2 are, therefore,

$$R_2 = (R_o^2 + r_2^2 + 2R_o r_2 \cos\alpha)^{1/2} \qquad (2.3.20)$$

$$V_2^2 = \dot{R}_o^2 + R_o^2 \dot{\theta}^2 + r_2^2 \dot{\theta}^2 (1+\alpha')^2 + 2 r_2 \dot{\theta} (1+\alpha') (R_o \dot{\theta} \cos\alpha - \dot{R}_o \sin\alpha) \qquad (2.3.21)$$

and similarly,

$$V_1^2 = \dot{R}_o^2 + R_o^2 \dot{\theta}^2 + r_1^2 \dot{\theta}^2 (1+\alpha')^2 + 2 r_1 \dot{\theta} (1+\alpha') (-R_o \dot{\theta} \cos\alpha + \dot{R}_o \sin\alpha) \qquad (2.3.22)$$

2.3.2 Final orbit parameters

The equations of motion as obtained in Sec. 2.2, viz.

$$\alpha'' - \left(\frac{2e \sin \theta}{1+e \cos \theta} \right) (\alpha' + 1) + \frac{3}{1 + e \cos \theta} \cos \alpha \sin \alpha = 0 \qquad (2.2.13)$$

can be solved numerically to yield α and α' at any θ for any set of given initial conditions. Then, from last subsection, V_2 and R_2 can be calculated and therefore specific energy (total energy per unit mass of body M_2) ϵ, becomes:

$$\epsilon = - \frac{\mu}{2a_2} = - \frac{\mu}{R_2} + \frac{V_2^2}{2} \qquad (2.3.23)$$

leading to[13]

$$a_2 = R_2 / \left[2 - \frac{R_2 V_2^2}{\mu} \right] \qquad (2.3.24)$$

and,

$$e_2 = \left\{ \left[\frac{R_2 V_2^2}{\mu} - 1 \right]^2 + \left[\frac{R_2 V_2^2}{\mu} \right] \left[2 - \frac{R_2 V_2^2}{\mu} \right] \cos^2 \beta \right\}^{1/2} \qquad (2.3.25)$$

where β is the angle between vectors $\vec{R}_2$ and $\vec{V}_2$, that is

$$\cos \beta = \frac{\vec{R}_2 \vec{V}_2}{R_2 V_2} \qquad (2.3.26)$$

2.4 AN APPROXIMATE ANALYTICAL SOLUTION

The equations of motion, given by Eq. (2.2.13) is a nonlinear second order differential equation. To get an analytical solution, we must be able to linearize it. Although linearization will obviously introduce some error, it is still useful in the

sense that we can get an insight into the basic nature of the problem.

$$\alpha'' - \left[\frac{2e \sin\theta}{1+e\cos\theta}\right](\alpha'+1) + \frac{3}{1+e\cos\theta}\cos\alpha\sin\alpha = 0 \qquad (2.2.13)$$

$$\rightarrow \quad \alpha'' - \left[\frac{2e\sin\theta\,\alpha'}{1+e\cos\theta}\right] + \frac{3}{1+e\cos\theta}\cos\alpha\sin\alpha = \frac{2e\sin\theta}{1+e\cos\theta}$$

Rearranging, we get,

$$(1 + e\cos\theta)\,\alpha'' - 2e\sin\theta\,\alpha' + 3\sin\alpha\cos\alpha = 2e\sin\theta \qquad (2.4.1)$$

We put,

$$(1 + e\cos\theta)\,\alpha = y \qquad (2.4.2)$$

therefore,

$$y' = (1 + e\cos\theta)\,\alpha' - e\sin\theta\,\alpha \qquad (2.4.3)$$

and

$$y'' = (1 + e\cos\theta)\,\alpha'' - 2e\sin\theta\,\alpha' - e\cos\alpha \qquad (2.4.4)$$

Thus, Eq. (2.4.1) becomes,

$$y'' + e\cos\theta\,\alpha + 3\sin\alpha\cos\alpha = 2e\sin\theta \qquad (2.4.5)$$

Assuming α to be small, so that

$$\sin\alpha \simeq \alpha \text{ and } \cos\alpha \simeq 1$$

this equation becomes,

$$y'' + (3 + e\cos\theta)\,\alpha = 2e\sin\theta \qquad (2.4.6)$$

Substituting α from Eq. (2.4.2), we get

$$y'' + \frac{(3 + e\cos\theta)y}{1 + e\cos\theta} = 2e\sin\theta \qquad (2.4.7)$$

For orbits with small eccentricity, e, we can write approximately from binomial expansion,

$$y'' + (3 - 2e \cos \theta)\, y = 2e \sin \theta \qquad (2.4.8)$$

which can be further simplified as

$$y'' + 3y = 2e \sin \theta \qquad (2.4.9)$$

This is a linear equation which has the following closed-form solution:

$$y = A \cos \sqrt{3}\, \theta + B \sin \sqrt{3}\, \theta + e \sin \theta \qquad (2.4.10)$$

where A and B are constants which depend upon initial conditions. If α_o and α_o' be the initial values for α and α' respectively, from Eq. (2.4.2), we have

$$y(0) = (1 + e)\, \alpha_o$$

so that, A becomes

$$A = (1 + e)\, \alpha_o \qquad (2.4.11)$$

Similarly, we can find

$$B = \frac{(1 + e)\, \alpha_o' - e}{\sqrt{3}} \qquad (2.4.12)$$

Putting these in Eq. (2.4.10), we get

$$\alpha = \frac{1}{1 + e \cos \theta} \left[A \cos \sqrt{3}\, \theta + B \sin \sqrt{3}\, \theta + e \sin \theta \right] \qquad (2.4.13)$$

Similarly,

$$\alpha' = \frac{1}{1 + e \cos \theta} \left[-\sqrt{3} A \sin \sqrt{3}\, \theta + \sqrt{3} B \cos \sqrt{3}\, \theta + e \cos \theta + e \sin \theta\, \alpha \right] \qquad (2.4.14)$$

These analytical expressions readily yield the instantaneous position and velocity vectors for the payload as given by Eq.

(2.3.15) and (2.3.19).

The analytical expression thus obtained for the total payload energy when evaluated at small intervals around an orbit enables us to determine the optimum "cut-off" location as well as its corresponding major axis gain.

2.5 NUMERICAL SOLUTION

2.5.1 Methodology

We solve numerically the second order differential equation (Eq. 2.2.13) using the NAG subroutine D02BHF. The values thus obtained are utilized to obtain the position and velocity of the payload to be released and hence the major axis of its final orbit in release. In addition, we want to evaluate exactly when the payload should be released so that the payload major axis is a maximum. It may be noted that the determination of the time of release comes down to the determination of the position of the centre of mass (its true anomaly, θ) of the entire tether system on the initial orbit when the payload is released. One such method has been described by Amier[10], but it is applied to essentially circular starting orbits. We now extend it for elliptic starting orbits.

2.5.2 Numerical Integration

To solve Eq. (2.2.13) numerically, it was reduced to two equivalent first order differential equations by letting

$$Y(1) = \alpha$$

and $$Y(2) = \alpha' \qquad (2.5.1)$$

so that we have

$$Y'(1) = Y(2)$$

$$Y'(2) = \frac{2\ e \sin\theta}{1+e\cos\theta}\ [Y(2) + 1] + \frac{3}{1+e\cos\theta} \cos\{Y(1)\} \sin\{Y(1)\} \qquad (2.5.2)$$

These equations were solved using Runge-Kutta-Mersion method to give α and α' for θ varying from 0 to 360 degrees. Runge-Kutta method is quite accurate for non-stiff equations and stiffness test shows that these equations are non-stiff so that a reasonable tolerance of $\sim 10^{-4}$ and 10^{-5} was assumed. With α and α' thus obtained, the position and velocity R_2 and V_2 can be readily calculated as given in Sec. 2.3. Therefore, the specific energy becomes

$$\epsilon = -\frac{\mu}{R_2} + \frac{V_2^2}{2} \qquad (2.5.3)$$

To maximize it, we must set,

$$\frac{d\epsilon}{d\theta} = 0$$

To calculate $d\epsilon/d\theta$, we proceed as,

$$\epsilon = -\frac{\mu}{R_2} + \frac{V_2^2}{2} \qquad (2.5.3)$$

Therefore,

$$\frac{d\epsilon}{d\theta} = V_2 \frac{dV_2}{d\theta} + \mu \frac{1}{R_2^2} \frac{dR_2}{d\theta} \qquad (2.5.4)$$

Eq. (2.3.20) gives the expression for R_2 as,

$$R_2^2 = R_o^2 + r_2^2 + 2R_o\, r_2 \cos\alpha$$

ifferentiating yields,

$$2R_2 \frac{dR_2}{d\theta} = 2R_o \dot{R}_o/\dot{\theta} + r_2^2 + 2r_2 (\dot{R}_o/\dot{\theta}) \cos\alpha + 2 R_o r_2 (-\sin\alpha)\alpha' \quad (2.5.5)$$

here dot denotes differentiation w.r.t. time and prime denotes ifferentiation w.r.t. θ. Thus the 2nd term on the right of Eq. 2.5.4) becomes

$$\frac{\mu}{R_2^2}\frac{dR_2}{d\theta} = \frac{\mu}{R_2\dot{\theta}}\left[R_o \dot{R}_o + \frac{r_2^2 \dot{\theta}}{2} + r_2 \dot{R}_o \cos\alpha - R_o r_2 \sin\alpha \alpha'\right] \quad (2.5.6)$$

R_o, R_2, θ and their derivatives are obtained from Eq. (2.3.5) to (2.3.11). Again, Eq. (2.3.21) gives,

$$V_2^2 = \dot{R}_2^2 + R_o^2 \dot{\theta}^2 + r_2^2 \dot{\theta}^2 (1+\alpha')^2 + 2r_2 \dot{\theta} (1+\alpha') [R_o \dot{\theta} \cos\alpha - \dot{R}_o \sin\alpha] \quad (2.5.7)$$

differentiation gives $2V_2 \frac{dV_2}{d\theta}$ on the left which is twice the first term on the right of Eq. (2.5.4). So, we divide each term on the right of (2.5.7) by two after differentiation and that gives us following five terms:

$$F(1) = \dot{R}_o \ddot{R}_o/\dot{\theta} \quad (2.5.8a)$$

$$F(2) = R_o \dot{R}_o \dot{\theta} + R_o^2 \ddot{\theta} \quad (2.5.8b)$$

$$F(3) = r_2^2 (1+\alpha')\left[\ddot{\theta}(1+\alpha') + \dot{\theta}^2 \alpha''\right] \quad (2.5.8c)$$

$$F(4) = r_2 \left[2R_o \dot{\epsilon} (1+\alpha') \cos\alpha + R_o \dot{\theta}^2 \alpha'' \cos\alpha - \dot{\theta}^2 (1+\alpha') \alpha' \sin\alpha R_o + \dot{\theta} (1+\alpha') \cos\alpha \dot{R}_o \right] \quad (2.5.8d)$$

$$F(5) = - r_2 \left[(\ddot{\theta}/\dot{\theta}) \dot{R}_o (1+\alpha') \sin\alpha + \ddot{k}_o (1+\alpha') \sin\alpha + \dot{\theta} \dot{R}_o \alpha'' \sin\alpha + \dot{\theta} \dot{R}_o (1+\alpha') \alpha' \cos\alpha \right] \quad (2.5.8e)$$

Here also, the derivatives of R_o and θ are obtained from Eq. (2.3.5) to (2.3.11) and thus,

$$V_2 \frac{dV_2}{d\theta} = F(1) + F(2) + F(3) + F(4) + F(5) \quad (2.5.9)$$

combining Eq. (2.5.6) and (2.5.9), we get the expression for $d\epsilon/d\theta$ in terms of α, α' and θ. Numerical solution of (2.5.2) gives α and α' for various θ. Our task is to find that θ for which $d\epsilon/d\theta$ (a function of α, α' and θ) becomes zero. Actually, this condition alone is not sufficient to guarantee the maximum. It gives several local extrema (both maxima and minima) but the total number of the local extrema is rather small (as can be seen from the next section). We numerically obtain the global maximum.

At $\theta = 0$, α and α' are known from initial conditions. We calculate $d\epsilon/d\theta$ using these values at initial point. Now, increasing θ by a small amount, δ, we obtain the new α, α' from the numerical integration of (2.5.2) and check for the sign change in $d\epsilon/d\theta$. If there is no sign change, we keep on increasing θ. Thus, we can bracket the range over which a sign change occurs. Then, the bracketed interval can be shortened by reducing δ. But

reducing δ also reduces the accuracy of α and α' obtained by numerical integration. We have to be judicious in the choice of tolerance, δ, so that the error stays within reasonable limits. We have used more than one value of tolerance to get reasonably accurate and constant results.

The above algorithm is used to set up a computer program to compute the various true-anomalies θ_r's where the payload should be released to reach the maximum or minimum possible altitudes. This enables us to obtain the maximum possible increase in the major axis of the payload on release alongwith the "cut-off" location.

2.6 RESULTS AND DISCUSSION

Numerical results are obtained for following parameters: $M_1 = 10^5$ kg, $M_2 = 500$ kg, $M_3 = 500$ kg, l (length of tether) = 100 km. R_p (perigee height) = 440 km. The time (or θ) is measured from the perigee passage. The radius of the Earth is assumed to be constant and equal to Re = 6378 km whereas $\mu = 3.986 \times 10^{14}$ m^3/s^2.

The tether system is assumed to enter its nominal orbit at the perigee with initial rotation α_o and initial velocity α_o' denoting the in-plane pitch-motion. The out-of-plane librations, such as roll,has not been considered because of its little effect on altitude gain as shown in earlier investigations.

With two tolerances of $\delta = 10^{-4}$ and 10^{-5}, the program runs are performed for different initial configurations of the tethered system. The tabulated results for the following configurations are presented from Table 2.1 to 2.10.

(i) $e = 0$; $\alpha_o = 0$; $\alpha_o' = 0, 0.05, 0.1, 0.2, 0.5$

(ii) $e = 0$; $\alpha_o' = 0$; $\alpha_o = 5.8, 18, 45, 60, 90$ degrees

(iii) $e = 0.01$; $\alpha_o' = 0$; $\alpha_o = 0, 5.8, 18, 45, 60, 90$ degrees

(iv) $e = 0.01$, $\alpha_o = 0$; $\alpha_o' = 0.01, 0.05, 0.1, 0.3$

(v) $e = 0.05$, $\alpha_o = 0$; $\alpha_o' = 0.02, 0.1, 0.3$

(vi) $e = 0.05$, $\alpha_o = 5.8$, $\alpha_o' = 0.01$

$\alpha_o = 45$, $\alpha_o' = 0.01$

$\alpha_o = 120$, $\alpha_o' = 0.3$

(vii) $e = 0.1$; $\alpha_o = 0$, $\alpha_o' = 0.02, 0.1, 0.3$

(viii) $e = 0.1$; $\alpha_o = 5.8$, $\alpha_o' = 0$

$\alpha_o = 45$, $\alpha_o' = 0.01$

$\alpha_o = 90$, $\alpha_o' = 0.05$

$\alpha_o = 120$, $\alpha_o' = 0.1$

(ix) $e = 0.5$; $\alpha_o = 0$, $\alpha_o' = 0.01$

$\alpha_o = 0$, $\alpha_o' = 0.1$

$\alpha_o = 10$, $\alpha_o' = 0$

$\alpha_o = 45$, $\alpha_o' = 0.001$

$\alpha_o = 90$, $\alpha_o' = 0.12$

Tables 2.2 and 2.3 list the results for a circular orbit, for which solutions are available from earlier investigations. As we find, our results are matching well. Bekey[8] and Amier[10] reported that if the release occurs while the payload is stable and along

than the perigee by about seven times the length of the tether. This so called "seven-times rule" for the non-librating system has been completely verified by our results. For circular orbits have been larger α_o' at $\theta = 0$ for systematically aligned with a local vertical leads to greater increase in the payload orbits.

Other notable features are, the gain in altitude, H_m, as well as the gain in the semi-major axis Δa, are much larger for initial orbits with high eccentricity, e. Again for the same e, the gain is more in the case of higher α_o' with system initially aligned. Thus initial pitch velocity is more important than the initial pitch angle.

CHAPTER III

TRANSVERSE VIBRATIONS OF THREE-BODY TETHERED SYSTEMS

3.1 DESCRIPTION OF THE SYSTEM

The tethered system under consideration consists of three bodies having masses m_1, m_2 and m_3 as shown in Fig. 3.1. The length of the tether connecting the end mass m_1 and the middle mass m_3 and the one connecting the end-mass m_2 and the middle mass are denoted by l_1 and l_2 respectively. The masses of the tether segments are m_{t1} and m_{t2} respectively. The angles α_1 and α_2 represent the inclinations of the tethers to the local vertical. The orbital coordinate system xyz is located at the system center of mass, as shown in the Fig. 3.1. CM is assumed to follow a circular orbit with orbital rate Ω. l_1 and l_2 are independent of each other and the system represents a three-body tethered constellation.

3.1.1 Equilibrium Configurations

Assuming fixed length of tethers, it can be shown, by suitable analysis of the librational motion of the system, that there are four possible equilibrium configurations. It can further be shown that only one of these configurations is stable. In this configuration, the masses are aligned with local vertical, as shown in the Fig. 3.2a. Here, the transverse vibrations of the system are considered for this stable equilibrium configuration.

3.1.2 Kinematics of the System

As the motion is in the orbital plane, the displacements are represented by the inplane coordinates y_i, z_i; for the three masses; i = 1,2,3. Furthermore, since CM is the centre of mass, the following constraint equations hold:

$$\sum_{i=1}^{3} m_i y_i = 0 \ , \quad \sum_{i=1}^{3} m_i z_i = 0$$

It should be noted that the tether masses are being neglected for this analysis. In the Fig. 3.2, we see that

$$z_1 < 0$$

$$z_2, z_3 > 0$$

also, $$z_3 = z_1 - l_1$$

$$z_2 = z_3 + l_2 = z_1 + l_1 + l_2$$

so that the 2nd of the constraint equations become:

$$m_1 z_1 + m_2 (z_1 + l_1 + l_2) + m_3 (z_1 + l_1) = 0$$

therefore,

$$(m_1 + m_2 + m_3) z_1 + (m_2 + m_3) l_1 + m_2 l_2 = 0$$

$$z_1 = - \frac{(m_2+m_3) l_1 + m_2 l_2}{m_1+m_2+m_3}$$

If we define mass ratios in the following way:

$$\bar{\mu}_i = \frac{m_i}{m} \quad ; \qquad i = 1,2,3 \qquad (3.1.1)$$

with $m = m_1 + m_2 + m_3$

then

$$z_1 = - (\bar{\mu}_2 + \bar{\mu}_3) l_1 - \bar{\mu}_2 l_2 \qquad (3.1.2a)$$

Similarly, $$z_2 = - \bar{\mu}_1 l_1 + (\bar{\mu}_2 + \bar{\mu}_3) l_2 \qquad (3.1.2b)$$

and $$z_3 = \bar{\mu}_1 l_1 - \bar{\mu}_2 l_2 \qquad (3.1.2c)$$

These equations can be rewritten in the following matrix - vector form:

$$\begin{Bmatrix} z_1 \\ z_2 \\ z_3 \end{Bmatrix} = [C] \begin{Bmatrix} l_1 \\ l_2 \end{Bmatrix} \qquad (3.1.3)$$

where,

$$[C] = \begin{bmatrix} -\bar{\mu}_2 \bar{\mu}_3 & -\bar{\mu}_2 \\ \bar{\mu}_1 & \bar{\mu}_1 \bar{\mu}_3 \\ \bar{\mu}_1 & \bar{\mu}_2 \end{bmatrix}$$

$$\begin{Bmatrix} y_1 \\ y_2 \\ y_3 \end{Bmatrix} = [C] \begin{Bmatrix} l_1 \alpha_1 \\ l_2 \alpha_2 \end{Bmatrix} \qquad (3.1.4)$$

3.1.3 Tensions in the Tether

Let T_1 and T_2 be the tension in the two tethers. Also, the distance of m_2 from the centre of Earth r_2 is given by

$$r_2 = R_c + z_2$$

where, R_c is the orbital radius of CM.

The free body diagram of m_2 and m_3 are shown in Fig. 3.2(b) and 3.2(c). From these we obtain

$$m_2 \ (-\omega^2 r_2) = -T_2 - \frac{\mu m_2}{r_2^2}$$

$$T_2 = m_2\omega^2 r_2 - \frac{\mu m_2}{R_2^2}\left(1 + \frac{z_2}{R_C}\right)^{-2}$$

expanding the last term in binomial series and neglecting higher order terms:

$$T_2 = m_2\omega^2 r_2 - \frac{\mu m_2}{R_2^2}\left(1 - 2\frac{z_2}{R_C} + \ldots\right)$$

using $\omega^2 = \frac{\mu}{R_c^3}$, we obtain

$$T_2 \approx 3m_2\omega^2 z_2$$

Putting z_2 in terms of mass ratios from Eq. (3.1.2b)

$$T_2 \approx 3(m\bar{\mu}_2)\omega^2 [\bar{\mu}_1 l_1 + (\bar{\mu}_1 + \bar{\mu}_3) l_2]$$

$$= 3m\omega^2 [\bar{\mu}_1 \bar{\mu}_2 l_1 + \bar{\mu}_2 (\bar{\mu}_1 + \bar{\mu}_3) l_2] \qquad (3.1.5)$$

Similarly, from Fig. 3.2(b)

$$m_3(-\omega^2 r_3) = T_2 - T_1 - \frac{\mu m_3}{r_3^2}$$

which leads to

$$T_1 \approx T_2 + 3m_3\omega^2 z_3$$

Putting the values of T_2 from Eq. (3.1.5) and z_3 from Eq. (3.1.2c) we obtain:

$$T_1 = 3m\omega^2 [\bar{\mu}_1 (\bar{\mu}_2 + \bar{\mu}_3) l_1 + \bar{\mu}_1 \bar{\mu}_2 l_2] \qquad (3.1.6)$$

3.2 MODELLING OF TRANSVERSE VIBRATIONS

Since for vibrating tether, like vibrating string, we cannot neglect its mass. So, we define new mass ratios, taking into account the tether masses. Thus,

$$\mu_i = \frac{m_i}{m} \quad i = 1,2,3$$

and $\mu_{t1} = \frac{m_{t1}}{m}$ $\mu_{t2} = \frac{m_{t2}}{m}$ (3.2.1)

where, $m = m_1 + m_2 + m_3 + m_{t1} + m_{t2}$ = total mass

Now, from Fig. 3.3, assuming small motions, we can write:

$$y_{t1} = y_1 - (y_1 - y_3)\,\xi_1 + u_1 \cos\alpha_1$$

$$\approx y_1\,(1 - \xi_1) + y_3\,\xi_1 + u_1\,(\xi_1, t)$$

where, ξ_1 is a nondimensional distance along the nominal tether line measured from the mass m_1, Fig. 3.3. Hence,

$$\xi_1 = 0 \text{ at } m_1 \quad \text{and} \quad \xi_1 = 1 \text{ at } m_3$$

Also, $u_1 = 0$ at $\xi_1 = 0$ and $\xi_1 = 1$

Similarly,

$$y_{t2} = y_2\,(1 - \xi_2) + y_3\,\xi_2 + u_2$$

where, ξ_2 is measured from mass m_2 and $0 \le \xi_2 \le 1$.

Also, $U_2\,(0, t) = U_2\,(1, t) = 0$

Now, from the definition of CM, we have

$$\sum_{i=1}^{3} m_i\,y_i + \sum_{i=1}^{2} \int_0^1 y_{ti}\,(m_{ti}\,d\xi_i) = 0$$

which leads to

$$(m_1 + \tfrac{1}{2}\,m_{t1})\,y_1 + (m_2 + \tfrac{1}{2}\,m_{t2})\,y_2 + (m_3 + \tfrac{1}{2}\,m_{t1} + \tfrac{1}{2}\,m_{t2})\,y_3 + m_{t1}\,U_1 + m_{t2}\,U_2 = 0$$

where $U_1 = \int_0^1 u_1\,d\xi_1$ and $U_2 = \int_0^1 u_2\,d\xi_2$

We now define,

$$y_1 = \hat{y}_1 + y_3 \; ; \quad y_2 = \hat{y}_2 + y_3$$

Then we can show

$$y_1 = \left[1 - \left\{ \mu_1 + \frac{1}{2} \mu_{t1} \right\} \right] \hat{y}_1 - \left\{ \mu_2 + \frac{1}{2} \mu_{t2} \right\} \hat{y}_2 - \mu_{t1} U_1 - \mu_{t2} U_2 \qquad (3.2.2a)$$

$$y_2 = \left[1 - \left\{ \mu_2 + \frac{1}{2} \mu_{t2} \right\} \right] \hat{y}_2 - \left\{ \mu_1 + \frac{1}{2} \mu_{t1} \right\} \hat{y}_1 - \mu_{t1} U_1 - \mu_{t2} U_2 \qquad (3.2.2b)$$

$$y_3 = - \left\{ \mu_1 + \frac{1}{2} \mu_{t1} \right\} \hat{y}_1 - \left\{ \mu_2 + \frac{1}{2} \mu_{t2} \right\} \hat{y}_2 - \mu_{t1} U_1 - \mu_{t2} U_2 \qquad (3.2.2c)$$

$$y_{t1} = \left[1 - \left\{ \mu_1 + \frac{1}{2} \mu_{t1} \right\} - \xi_1 \right] \hat{y}_1 - \left\{ \mu_2 + \frac{1}{2} \mu_{t2} \right\} \hat{y}_2 - \mu_{t1} U_1 - \mu_{t2} U_2 + u_1 \qquad (3.2.2d)$$

$$y_{t2} = \left[1 - \left\{ \mu_2 + \frac{1}{2} \mu_{t2} \right\} - \xi_2 \right] \hat{y}_2 - \left\{ \mu_1 + \frac{1}{2} \mu_{t1} \right\} \hat{y}_1 - \mu_{t1} U_1 - \mu_{t2} U_2 + u_2 \qquad (3.2.2e)$$

3.3 KINETIC ENERGY OF THE SYSTEM

The kinetic energy (KE) is given by

$$K = \frac{1}{2} \sum_{i=1}^{3} m_i \left(\dot{y}_i + \dot{z}_i \right)^2 + \frac{1}{2} \sum_{i=1}^{2} \int_0^1 \left(m_{ti} \, d\xi_i \right) \left(\dot{y}_{ti}^{\,2} + \dot{z}_{ti}^{\,2} \right)$$

For small transverse motion considered here, the KE associated with displacement components in the z-direction is negligible. However, the potential energy due to this cannot be neglected. So, we take into account the contribution due to motion in the z-direction in the calculation of PE in next

section. Thus, KE is

$$K \simeq \frac{1}{2} \sum_{i=1}^{3} m_i \dot{y}_i^2 + \frac{1}{2} \sum_{i=1}^{2} m_{ti} \int_0^1 \dot{y}_{ti}^2 \, d\xi_i$$

$$= \frac{m}{2} \sum_{i=1}^{3} \mu_i \dot{y}_i^2 + \frac{m}{2} \sum_{i=1}^{2} \mu_{ti} \int_0^1 \dot{y}_{ti}^2 \, d\xi_i$$

Substituting the expressions for y_i and y_{ti} obtained earlier, we get K in the following form:

$$\begin{aligned} K = \frac{m}{2} \Bigg[& a_{11} \dot{\tilde{y}}_1^2 + a_{22} \dot{\tilde{y}}_2^2 + a_{33} \dot{U}_1^2 + a_{44} \dot{U}_2^2 + a_{55} \int_0^1 \dot{u}_1^2 \, d\xi_1 \\ & + a_{66} \int_0^1 \dot{u}_2^2 \, d\xi_2 + 2a_{12} \dot{\tilde{y}}_1 \dot{\tilde{y}}_2 + 2a_{13} \dot{\tilde{y}}_1 \dot{U}_1 + 2a_{14} \dot{\tilde{y}}_1 \dot{U}_2 \\ & + 2 \dot{\tilde{y}}_2 \left[a_{15} \dot{U}_1 + \bar{a}_{15} \int_0^1 \xi_1 \dot{u}_1 \, d\xi_1 \right] + 2 a_{16} \dot{\tilde{y}}_1 \dot{U}_2 \\ & + 2 a_{23} \dot{\tilde{y}}_2 \dot{U}_1 + 2 a_{24} \dot{\tilde{y}}_2 \dot{U}_2 + 2 a_{25} \dot{\tilde{y}}_2 \dot{U}_1 \\ & + 2 \dot{\tilde{y}}_2 \left[a_{26} \dot{U}_2 + \bar{a}_{26} \int_0^1 \xi_2 \dot{u}_2 \, d\xi_2 \right] + 2 a_{34} \dot{U}_1 \dot{U}_2 \\ & + 2 a_{35} \dot{U}_1^2 + 2 a_{36} \dot{U}_1 \dot{U}_2 + 2 a_{45} \dot{U}_2 \dot{U}_1 + 2 a_{46} \dot{U}_2^2 \Bigg] \end{aligned} \quad (3.3.1)$$

where, a_{11} etc. are functions of mass ratios. For example,

$$\begin{aligned} a_{11} = & \mu_1 \left[1 - (\mu_1 + \tfrac{1}{2} \mu_{t1}) \right]^2 + \mu_2 (\mu_1 + \tfrac{1}{2} \mu_{t1})^2 \\ & + \mu_3 (\mu_1 + \tfrac{1}{2} \mu_{t1})^2 + \mu_{t1} \int_0^1 \left[1 - (\mu_1 + \tfrac{1}{2} \mu_{t1}) - \xi_1 \right]^2 d\xi_1 \\ & + \mu_{t2} (\mu_1 + \tfrac{1}{2} \mu_{t1})^2 \end{aligned}$$

$$= (\mu_1 + \tfrac{1}{2}\mu_{t1})^2 (\mu_1 + \mu_2 + \mu_3 + \mu_{t2}) + \mu_1 \left[1-2(\mu_1 + \tfrac{1}{2}\mu_{t1}) \right]$$

$$+ \mu_{t1} \left[\tfrac{1}{3} - (\mu_1 + \tfrac{1}{2}\mu_{t1}) + (\mu_1 + \tfrac{1}{2}\mu_{t1})^2 \right]$$

$$= (\mu_1 + \tfrac{1}{2}\mu_{t1})^2 (\mu_1 + \mu_2 + \mu_3 + \mu_{t1} + \mu_{t2}) + (\mu_1 + \tfrac{1}{3}\mu_{t1})$$

$$- (\mu_1 + \tfrac{1}{2}\mu_{t1}) (2\mu_1 + \mu t_1)$$

$$= (\mu_1 + \tfrac{1}{2}\mu_{t1})^2 + (\mu_1 + \tfrac{1}{3}\mu_{t1}) - 2 (\mu_1 + \tfrac{1}{2}\mu_{t1})^2$$

Therefore,

$$a_{11} = (\mu_1 + \tfrac{1}{3}\mu_{t1}) - (\mu_1 + \tfrac{1}{2}\mu_{t1})^2 \qquad (3.3.2a)$$

Similarly,

$$a_{22} = (\mu_2 + \tfrac{1}{3}\mu_{t2}) - (\mu_2 + \tfrac{1}{2}\mu_{t2})^2 \qquad (3.3.2b)$$

$$a_{33} = \mu_{t1}^2 \qquad (3.3.2c)$$

$$a_{44} = \mu_{t2}^2 \qquad (3.3.2d)$$

$$a_{55} = \mu_{t1} \qquad (3.3.2e)$$

$$a_{66} = \mu_{t2} \qquad (3.3.2f)$$

And,

$$-a_{12} = \mu_1 \left[1 - (\mu_1 + \tfrac{1}{2}\mu_{t1}) \right] (\mu_2 + \tfrac{1}{2}\mu_{t2})$$

$$+ \mu_2 \left[1 - (\mu_2 + \tfrac{1}{2}\mu_{t2}) \right] (\mu_1 + \tfrac{1}{2}\mu_{t1})$$

$$- \mu_3 (\mu_1 + \tfrac{1}{2}\mu_{t1}) (\mu_2 + \tfrac{1}{2}\mu_{t2})$$

$$+ \mu_{t1} (\mu_2 + \tfrac{1}{2}\mu_{t2}) \int_0^1 \left[1 - (\mu_1 + \tfrac{1}{2}\mu_{t1}) - \xi_1 \right] d\xi_1$$

$$+ \mu_{t2} (\mu_1 + \tfrac{1}{2}\mu_{t1}) \int_0^1 \left[1 - (\mu_2 + \tfrac{1}{2}\mu_{t2}) - \xi_2 \right] d\xi_2$$

$$= \mu_1 (\mu_2 + \tfrac{1}{2}\mu_{t2}) + \mu_2 (\mu_1 + \tfrac{1}{2}\mu_{t1})$$

$$+ \tfrac{1}{2}\mu_{t1} (\mu_2 + \tfrac{1}{2}\mu_{t2}) + \tfrac{1}{2}\mu_{t2} (\mu_1 + \tfrac{1}{2}\mu_{t1})$$

$$+ (\mu_1 + \tfrac{1}{2}\mu_{t1}) (\mu_2 + \tfrac{1}{2}\mu_{t2}) [- \mu_1 - \mu_2 - \mu_3 - \mu_{t1} - \mu_{t2}]$$

$$= 2 (\mu_1 + \tfrac{1}{2}\mu_{t1}) (\mu_2 + \tfrac{1}{2}\mu_{t2}) - (\mu_1 + \tfrac{1}{2}\mu_{t1}) (\mu_2 + \tfrac{1}{2}\mu_{t2})$$

Therefore,

$$a_{12} = - (\mu_1 + \tfrac{1}{2}\mu_{t1}) (\mu_2 + \tfrac{1}{2}\mu_{t2}) \qquad (3.3.2g)$$

Again,

$$a_{13} = - \mu_1 \left[1 - (\mu_1 + \tfrac{1}{2}\mu_{t1})\right] \mu_{t1} + \mu_2 (\mu_1 + \tfrac{1}{2}\mu_{t1}) \mu_{t1}$$

$$+ \mu_3 (\mu_1 + \tfrac{1}{2}\mu_{t1}) \mu_{t1}$$

$$- \mu_{t1}^2 \int_0^1 \left[1 - (\mu_1 + \tfrac{1}{2}\mu_{t1}) - \xi_1 \right] d\xi_1$$

$$+ \mu_{t2} (\mu_1 + \tfrac{1}{2}\mu_{t1}) \mu_{t1}$$

$$= (\mu_1 + \tfrac{1}{2}\mu_{t1}) \mu_{t1} [\mu_1 + \mu_2 + \mu_3 + \mu_{t1} + \mu_{t2}]$$

$$- \mu_1 \mu_{t1} - \mu_{t1}^2 \tfrac{1}{2}$$

$$= (\mu_1 + \tfrac{1}{2}\mu_{t1}) \mu_{t1} - \mu_{t1} (\mu_1 + \tfrac{1}{2}\mu_{t1}) = 0$$

(3.3.2h)

$$a_{14} = -\mu_1 \left[1 - (\mu_1 + \tfrac{1}{2}\mu_{t1})\right] \mu_{t2} + \mu_2 (\mu_1 + \tfrac{1}{2}\mu_{t1}) \mu_{t2}$$

$$+ \mu_3 (\mu_1 + \tfrac{1}{2}\mu_{t1}) \mu_{t2}$$

$$- \mu_{t1} \int_0^1 \left[1 - (\mu_1 + \tfrac{1}{2}\mu_{t1}) - \xi_1 \right] d\xi_1 \mu_{t2}$$

$$+ \mu_{t2} (\mu_1 + \tfrac{1}{2}\mu_{t1}) \mu_{t2}$$

$$= (\mu_1 + \tfrac{1}{2}\mu_{t1}) \mu_{t2} [\mu_1 + \mu_2 + \mu_3 + \mu_{t1} + \mu_{t2}]$$

$$- \mu_1 \mu_{t2} - \mu_{t1} \tfrac{1}{2} \mu_{t2}$$

$$= (\mu_1 + \tfrac{1}{2}\mu_{t1}) \mu_{t2} - \mu_{t2} (\mu_1 + \tfrac{1}{2}\mu_{t1}) = 0$$

(3.3.2i)

$$a_{15} = \mu_{t1} \left[1 - (\mu_1 + \tfrac{1}{2}\mu_{t1}) \right] \qquad (3.3.2j)$$

$$\bar{a}_{15} = -\mu_{t1} \qquad (3.3.2k)$$

$$a_{16} = -\mu_{t2} (\dot{\mu}_1 + \tfrac{1}{2}\mu_{t1}) \qquad (3.3.2l)$$

Now,

$$a_{23} = \mu_1 (\mu_2 + \tfrac{1}{2}\mu_{t2}) \mu_{t1} - \mu_2 \left[1 - (\mu_2 + \tfrac{1}{2}\mu_{t2}) \right] \mu_{t1}$$

$$+ \mu_3 (\mu_2 + \tfrac{1}{2}\mu_{t2}) \mu_{t1} + \mu_{t1} (\mu_2 + \tfrac{1}{2}\mu_{t2}) \mu_{t1}$$

$$- \mu_{t2} \mu_{t1} \int_0^1 \left[1 - (\mu_2 + \tfrac{1}{2}\mu_{t2}) - \xi_2 \right] d\xi_2$$

$$= (\mu_2 + \tfrac{1}{2}\mu_{t2}) \mu_{t1} [\mu_1 + \mu_2 + \mu_3 + \mu_{t1} + \mu_{t2}]$$

$$- \mu_2 \mu_{t1} - \mu_{t2} \frac{1}{2} \mu_{t1}$$

$$= 0 \qquad (3.3.2m)$$

$$a_{24} = \mu_1 (\mu_2 + \frac{1}{2} \mu_{t2}) \mu_{t2} - \mu_2 \left[1 - (\mu_2 + \frac{1}{2} \mu_{t2}) \right] \mu_{t2}$$

$$+ \mu_3 (\mu_2 + \frac{1}{2} \mu_{t2}) \mu_{t2} + \mu_{t1} (\mu_2 + \frac{1}{2} \mu_{t2}) \mu_{t2}$$

$$- \mu_{t2} \mu_{t2} \int_0^1 \left[1 - (\mu_2 + \frac{1}{2} \mu_{t2}) - \xi_2 \right] d\xi_2$$

$$= 0 \qquad (3.3.2n)$$

$$a_{25} = - \mu_{t1} (\mu_2 + \frac{1}{2} \mu_{t2}) \qquad (3.3.2o)$$

$$a_{26} = \mu_{t2} \left[1 - (\mu_2 + \frac{1}{2} \mu_{t2}) \right] , \qquad (3.3.2p)$$

$$\bar{a}_{26} = - \mu_{t2} \qquad (3.3.2q)$$

Also,

$$a_{34} = \mu_{t1} \mu_{t2} \qquad (3.3.2r)$$

$$a_{35} = - \mu_{t1}^2 \qquad (3.3.2s)$$

$$a_{36} = - \mu_{t1} \mu_{t2} \qquad (3.3.2t)$$

$$a_{45} = - \mu_{t1} \mu_{t2} \qquad (3.3.2u)$$

$$a_{46} = - \mu_{t2}^2 \qquad (3.3.2v)$$

We can combine few terms as:

$$a_{33} + 2 a_{35} = - \mu_{t1}^2 \qquad (3.3.2w)$$

$$a_{44} + 2 a_{46} = - \mu_{t2}^2 \qquad (3.3.2x)$$

$$a_{34} + a_{36} + a_{45} = - \mu_{t1}\, \mu_{t2} \qquad (3.3.2y)$$

Putting (3.3.2a) to (3.3.2y) in (3.3.1), we obtain

$$\begin{aligned}
\frac{K}{m/2} = & \left\{ (\mu_1 + \tfrac{1}{3}\mu_{t1}) - (\mu_1 + \tfrac{1}{2}\mu_{t1})^2 \right\} \dot{\bar{y}}_1^{\,2} \\
& + \left\{ (\mu_2 + \tfrac{1}{3}\mu_{t2}) - (\mu_2 + \tfrac{1}{2}\mu_{t2})^2 \right\} \dot{\bar{y}}_2^{\,2} \\
& - 2\,(\mu_1 + \tfrac{1}{2}\mu_{t1})\,(\mu_2 + \tfrac{1}{2}\mu_{t2})\, \dot{\bar{y}}_1\, \dot{\bar{y}}_2 \\
& + \mu_{t1} \int_0^1 \dot{u}_1^{\,2}\, d\xi_1 + \mu_{t2} \int_0^1 \dot{u}_2^{\,2}\, d\xi_2 \\
& - (\mu_{t1}\, \dot{U}_1 + \mu_{t2}\, \dot{U}_2)^2 + 2\, \dot{\bar{y}}_1 \left[\mu_{t1} \left\{ 1 - (\mu_1 + \tfrac{1}{2}\mu_{t1}) \right\} \dot{U}_1 \right. \\
& \left. - \mu_{t1} \int_0^1 \xi_1\, \dot{u}_1\, d\xi_1 - \mu_{t2}\, (\mu_1 + \tfrac{1}{2}\mu_{t1})\, \dot{U}_2 \right] \\
& + 2\, \dot{\bar{y}}_2 \left[\mu_{t2} \left\{ 1 - (\mu_2 + \tfrac{1}{2}\mu_{t2}) \right\} \dot{U}_2 \right. \\
& \left. - \mu_{t2} \int_0^1 \xi_2\, \dot{u}_2\, d\xi_2 - \mu_{t2}\, (\mu_2 + \tfrac{1}{2}\mu_{t2})\, \dot{U}_1 \right]
\end{aligned} \qquad (3.3.3)$$

We put,

$$u_1 = \sum_{i=1}^{n_1} q_{i1}(t)\, \phi_{i1}(\xi_1)$$

and

$$u_2 = \sum_{i=1}^{n_2} q_{i2}(t)\, \phi_{i2}(\xi_2)$$

therefore,

$$U_1 = \int_0^1 u_1 d\, \xi_1 = \sum_{i=1}^{n_1} q_{i1}(t) \int_0^1 \phi_{i1}(\xi_1)\, d\xi_1$$

We choose,

$$\phi_{i1} = \sqrt{2} \sin i \pi \xi_1 \text{ and } \phi_{i2} = \sqrt{2} \sin i \pi \xi_2$$

so that,

$$\int_0^1 \sqrt{2} \sin i \pi \xi_1 \, d\xi_1 = \begin{cases} 0 & \text{for even } i = 2, 4, 6, \ldots \\ \frac{2\sqrt{2}}{i\pi} & \text{for odd } i = 1, 3, 5, \ldots \end{cases}$$

therefore,

$$\dot{U}_1 = \sum_{i=1,3,..}^{n_1} \dot{q}_{i1}(t) \frac{2\sqrt{2}}{i\pi}$$

Similarly,

$$\dot{U}_2 = \sum_{i=1,3,..}^{n_2} \dot{q}_{i2}(t) \frac{2\sqrt{2}}{i\pi}$$

Now,

$$\int_0^1 \dot{u}_1^2 \, d\xi_1 = \sum_{i=1}^{n_1} \dot{q}_{i1}^2(t) \; ;$$

$$\int_0^1 \dot{u}_2^2 \, d\xi_2 = \sum_{i=1}^{n_1} \dot{q}_{i2}^2(t)$$

Again,

$$\int_0^1 \xi_1 \dot{u}_1 \, d\xi_1 = \sum_{i=1}^{n_1} (-1)^i \sqrt{2} \; \dot{q}_{i1}(t) \; ;$$

$$\int_0^1 \xi_2 \dot{u}_2 \, d\xi_2 = \sum_{i=1}^{n_2} (-1)^i \sqrt{2} \; \dot{q}_{i2}(t)$$

Putting these, we get KE as,

$$K = \frac{1}{2} m \left[a_{11} \dot{y}_1^2 + a_{22} \dot{y}_2^2 + a_{12} \dot{y}_1 \dot{y}_2 + \sum_{i=1}^{n_1} a_{i+2,i+2} \dot{q}_{i1}^2 \right.$$

$$+ \sum_{i=1}^{n_2} a_{i+n_1+2,i+n_1+2}\, \dot{q}_{i2}^{\,2} + 2 \sum_{i=1}^{n_1} a_{1,i+2}\, \dot{\bar{y}}_1\, \dot{q}_{i1}$$

$$+ 2 \sum_{i=1}^{n_2} a_{1,i+n_1+2}\, \dot{\bar{y}}_1\, \dot{q}_{i2} + 2 \sum_{i=1}^{n_1} a_{2,i+2}\, \dot{\bar{y}}_2\, \dot{q}_{i1}$$

$$+ 2 \sum_{i=1}^{n_2} a_{2,i+n_1+2}\, \dot{\bar{y}}_2\, \dot{q}_{i2} + 2 \sum_{i=1}^{n_1} \sum_{j=1}^{n_2} a_{2+i,n_1+2+j}\, \dot{q}_{i1}\, \dot{q}_{j2} \Big]$$

where,

$$a_{11} = (\mu_1 + \tfrac{1}{3}\mu_{t1}) - (\mu_1 + \tfrac{1}{2}\mu_{t1})^2$$

$$a_{22} = (\mu_2 + \tfrac{1}{3}\mu_{t2}) - (\mu_2 + \tfrac{1}{2}\mu_{t2})^2$$

$$a_{12} = -(\mu_1 + \tfrac{1}{2}\mu_{t1})(\mu_2 + \tfrac{1}{2}\mu_{t2})$$

$$a_{i+2,i+2} = \begin{cases} \mu_{t1}\,(1-8\mu_{t1}/i\pi) ; & i = 1,3,5, \ldots, n_1 \\ \mu_{t1} ; & i = 2,4,6, \ldots, n_1 \end{cases}$$

$$a_{i+n_1+2,i+n_1+2} = \begin{cases} \mu_{t2}\,(1-8\mu_{t2}/i\pi) ; & i = 1,3,5, \ldots, n_2 \\ \mu_{t2} ; & i = 2,4,6, \ldots, n_2 \end{cases}$$

$$a_{1,i+2} = \begin{cases} \mu_{t1}[(1-(\mu_1+\mu_{t1}/2))\,(2\sqrt{2}/i\pi) + \sqrt{2}]; & i = 1,3,..n_1 \\ \mu_{t1}\,(-\sqrt{2}) ; & i = 2,4,..n_1 \end{cases}$$

$$a_{2,i+2} = \begin{cases} \mu_{t2}[(1-(\mu_2+\mu_{t2}/2))\,(2\sqrt{2}/i\pi) + \sqrt{2}]; & i = 1,3,..n_1 \\ \mu_{t2}\,(-\sqrt{2}) ; & i = 2,4,..n_1 \end{cases}$$

$$a_{1,i+n_1+2} = \begin{cases} -\mu_{t2}\,(\mu_1+\mu_{t1}/2)\,(2\sqrt{2}/i\pi) + \sqrt{2}; & i = 1,3,..n_2 \\ 0 ; & i = 2,4,..n_2 \end{cases}$$

$$a_{2,i+n_1+2} = \begin{cases} -\mu_{t1}\ (\mu_2+\mu_{t2}/2)\ (2\sqrt{2}/i\pi) + \sqrt{2}; & i = 1,3,..n_2 \\ 0 & ; \ i = 2,4,..n_2 \end{cases}$$

$$a_{2+i,n_1+2+j} = \begin{cases} -\mu_{t1}\ \mu_{t2}\ (8/ij\pi^2) & ; \ i \text{ and } j = 1,3,.. \\ 0 & ; \ i \text{ and } j = 2,4,.. \end{cases}$$

Hence the mass matrix is given by

$$[M] = m\,[A] \qquad (3.3.4)$$

where, [A] is a square matrix of size (n_1+n_2+2) and is given by

$$[A] = \begin{bmatrix} a_{11} & a_{12} & -- & a_{1,n_1+2} & -- & a_{1,n_1+n_2+2} \\ & a_{22} & -- & a_{2,n_1+2} & -- & a_{2,n_1+n_2+2} \\ & & . & & & \\ & \text{Sym.} & & . & & \\ & & & & . & \end{bmatrix}.$$

3.4 POTENTIAL ENERGY OF THE SYSTEM

Potential energy, V, of the system has two parts, namely, gravitational and the elastic P.E.

$$V = V_g + V_e \qquad (3.4.1)$$

Again the gravitational P.E. is given by the sum of the gravitational P.E. of three masses and of two tethers. Of course, we neglect the tether deformations.

$$V_g = -\sum_{i=1}^{3} \frac{\mu\, m_i}{|\bar{R}_c + \bar{r}_i|} - \sum_{i=1}^{2} \frac{\mu\, m_{ti}}{|\bar{R}_c + \bar{r}_i|}$$

$$-\sum_{i=1}^{3} \mu\, m_i\, [(R_c\,\bar{j} + \bar{r}_i)\,(R_c\,\bar{j} + \bar{r}_i)]^{-1/2}$$

$$- \sum_{i=1}^{2} \mu\, m_{ti}\, [(R_c\, \bar{j} + \bar{r}_{ti})\, (R_c\, \bar{j} + \bar{r}_{ti})]^{-1/2}$$

By expanding the right hand side in a binomial series and ignoring terms higher than third order, it can be shown that

$$V_g = - \frac{\mu}{R_c}\, m - \frac{\mu}{R_c^{\,2}}\, \bar{j} \cdot \sum_{i=1}^{3} m_i\, \bar{r}_i$$

$$+ \frac{1}{2}\, \frac{\mu}{R_c^{\,3}} \sum_{i=1}^{3} m_i (\bar{r}_i \cdot \bar{r}_i - 3\, (\bar{j} \cdot \bar{r}_i)^2)$$

$$- \frac{\mu}{R_c^{\,2}}\, \bar{j} \cdot \sum_{i=1}^{2} m_{ti}\, \bar{r}_{ti} + \frac{1}{2}\, \frac{\mu}{R_c^{\,3}}$$

$$\sum_{i=1}^{3} m_{ti} (\bar{r}_{ti} \cdot \bar{r}_{ti} - 3\, (\bar{j} \cdot \bar{r}_{ti})^2)$$

Where the first term corresponds to the orbital P.E. of the system while the second and fourth terms vanish by virtue of the CM being the local frame origin. For remaining terms writing $\bar{r}_i$ and $\bar{r}_{ti}$ in terms of y_i and z_i and after some algebra, we finally get:

$$V_g = V_{gorb} + \frac{\mu}{2R_c^{\,3}} \left[\left\{ (\mu_1 + \tfrac{1}{3}\mu_{t1}) - (\mu_1 + \tfrac{1}{2}\mu_{t1})^2 \right\} \mu^2\, (1 - 3\cos^2 \alpha_1) \right.$$

$$+ \left\{ (\mu_2 + \tfrac{1}{3}\mu_{t2}) - (\mu_2 + \tfrac{1}{2}\mu_{t2})^2 \right\} \mu^2\, (1 - 3\cos^2 \alpha_2)$$

$$+ 2\, (\mu_1 + \tfrac{1}{3}\mu_{t1})\, (\mu_2 + \tfrac{1}{2}\mu_{t2})\, l_1\, l_2$$

$$\left. \left\{ \cos (\alpha_1 - \alpha_2) - 3 \cos \alpha_1 \cos \alpha_2 \right\} \right]$$

Now, $l_1 \alpha_1 = \hat{y}_1$, $l_2 \alpha_2 = -\hat{y}_2$

so that with a second order approximation for $\cos \alpha_1$ and $\cos \alpha_2$, i.e.,

$$\cos \alpha_1 \approx 1 - \alpha_1^2$$

$$\cos \alpha_2 \approx 1 - \alpha_2^2$$

we have

$$l_1^2 (1-3 \cos^2 \alpha_1) = -2 l_1^2 + 3 \hat{y}_1^2$$

$$l_2^2 (1 - 3 \cos^2 \alpha_2) = -2 l_2^2 + 3 \hat{y}_2^2$$

and

$$l_1 l_2 \left\{ \cos (\alpha_1 - \alpha_2) - 3 \cos \alpha_1 \cos \alpha_2 \right\}$$

$$= \left[- \hat{y}_1 \hat{y}_2 - 2 l_1 l_2 + \frac{l_1}{l_2} \hat{y}_2^2 + \frac{l_2}{l_1} \hat{y}_1^2 \right]$$

Utilizing these, we get

$$V_g = V_{gorb} + \frac{\Omega^2 m}{2} \left[\left\{ (\mu_1 + \frac{1}{3} \mu_{t1}) - (\mu_1 + \frac{1}{2} \mu_{t1})^2 \right\} (-2 l_1^2) \right.$$

$$+ \left\{ (\mu_2 + \frac{1}{3} \mu_{t2}) - (\mu_2 + \frac{1}{2} \mu_{t2})^2 \right\} (-2 l_2^2)$$

$$+ \hat{y}_1^2 \left\{ 3 \left\{ (\mu_1 + \frac{1}{3} \mu_{t1}) - (\mu_1 + \frac{1}{2} \mu_{t1})^2 \right\} \right.$$

$$+ \frac{2 l_1}{l_2} \left\{ (\mu_1 + \frac{1}{2} \mu_{t1}) - (\mu_1 + \frac{1}{2} \mu_{t1})^2 \right\}$$

$$+ \hat{y}_2^2 \left\{ 3 \left\{ (\mu_2 + \frac{1}{3} \mu_{t2}) - (\mu_2 + \frac{1}{2} \mu_{t2})^2 \right\} \right.$$

$$+ \frac{2 l_2}{l_1} \left\{ (\mu_1 + \frac{1}{2} \mu_{t1}) - (\mu_2 + \frac{1}{2} \mu_{t2})^2 \right\}$$

$$- 2 \hat{y}_1 \hat{y}_2 \left\{ (\mu_1 + \frac{1}{2} \mu_{t1}) - (\mu_2 + \frac{1}{2} \mu_{t2}) \right\}$$

$$+ 4\, l_1\, l_2 \left\{ (\mu_1 + \tfrac{1}{2}\mu_{t1}) - (\mu_2 + \tfrac{1}{2}\mu_{t2}) \right\} \qquad (3.4.2)$$

Now,

V_e = elastic strain energy stored in the tethers

$$= \frac{1}{2} \int_{\rho_1=0}^{l_1} T_1 \left(\frac{\partial u_1}{\partial \xi_1} \right)^2 ds_1 + \frac{1}{2} \int_0^{l_2} T_2 \left(\frac{\partial u_2}{\partial \xi_2} \right)^2 ds_2$$

$$= \frac{1}{2} \int_0^1 T_1 \left(\frac{1}{l_1^2} \right) \left(\frac{\partial u_1}{\partial \xi_1} \right)^2 l_1 \, d\xi_1$$

$$+ \frac{1}{2l_1} \int_0^1 T_1 \left(\frac{\partial u_1}{\partial \xi_1} \right)^2 d\xi_1 + \frac{1}{2l_2} \int_0^1 T_2 \left(\frac{\partial u_2}{\partial \xi_2} \right)^2 d\xi_2$$

Using the tension expressions given by Eq. (3.1.6)

$$V_e = \frac{3m\omega^2}{2} \left[\int_0^1 \left\{ \bar{\mu}_1 (\bar{\mu}_2 + \bar{\mu}_3) + \bar{\mu}_1 \bar{\mu}_2 \frac{l_2}{l_1} \right\} \left(\frac{\partial u_1}{\partial \xi_1} \right)^2 d\xi_1 \right.$$

$$\left. + \int_0^1 \left\{ \bar{\mu}_1 \bar{\mu}_2 \frac{l_1}{l_2} \bar{\mu}_2 (\bar{\mu}_1 + \bar{\mu}_3) \right\} \left(\frac{\partial u_2}{\partial \xi_2} \right)^2 d\xi_2 \right] \qquad (3.4.3)$$

To discretize, we use the same relations as in K.E. and get the following:

$$u_1 = \sum_{i=1}^{n_1} q_{i1}(t)\, \phi_{i1}(\xi_1) = \sum_{i=1}^{n_1} q_{i1}(t) \sqrt{2} \sin i\pi \xi_1$$

and

$$\frac{\partial u_1}{\partial \xi_1} = \sum_{i=1}^{n_i} q_{i1}^2(t) \frac{2}{i^2\pi^2} (1 + \cos 2i\pi \xi_1)$$

therefore,

$$\int_0^1 \left(\frac{\partial u_1}{\partial \xi_1} \right)^2 d\xi_1 = \sum_{i=1}^{n_1} q_{i1}^2(t) \frac{1}{i^2\pi^2} \int_0^1 (1 + \cos 2i\pi)\, d\xi_1$$

but $\int_0^1 (1 + \cos 2i\pi\, \xi_1)\, d\xi_1 = 1 + \frac{1}{2i\pi} \sin 2i\pi\, \xi_1 \Big|_0^1 = 1$

$$= \sum_{i=1}^{n_1} \frac{1}{i^2\pi^2} q_{i1}^2(t)$$

similarly,

$$\int_0^1 \left(\frac{\partial u_2}{\partial \xi_2} \right)^2 d\xi_2 = \sum_{i=1}^{n_2} \frac{1}{i^2\pi^2} q_{i1}^2(t)$$

Hence,

$$V_e = \frac{3m\omega^2}{2} \left\{ \bar{\mu}_1 (\bar{\mu}_2 + \bar{\mu}_3) + \frac{\bar{\mu}_1 \bar{\mu}_2 l_2}{l_2} \right\} \sum_{i=1}^{n_1} \frac{1}{i^2\pi^2} q_{i1}^2(t)$$

$$+ \left\{ \bar{\mu}_1 \bar{\mu}_2 \frac{l_1}{l_2} + \bar{\mu}_2 (\bar{\mu}_1 + \bar{\mu}_3) \right\} \sum_{i=1}^{n_1} \frac{1}{i^2\pi^2} q_{i1}^2(t) \qquad (3.4.4)$$

Putting (3.4.2) and (3.4.4) into (3.4.1), we get,

$$V = V_e + V_g = \frac{m\omega^2}{2} \left[b_{11} \hat{y}_1^2 + b_{22} \hat{y}_2^2 + 2b_{12} \hat{y}_1 \hat{y}_2 \right.$$

$$\left. + \sum_{i=1}^{n_1} b_{i+2,i+2} q_{i1}^2(t) + \sum_{i=1}^{n_2} b_{i,n_1+2,i+n_1+2} q_{i2}^2 \right] + C \qquad (3.4.5)$$

where C is a const. term (V_{gorb} etc.) which does not depend upon any of the generalized co-ordinates so they cancel up while differentiating in Lagrange's Eq. $\left\{\left[\left(\frac{\partial V}{\partial c}\right)\right.\right.$ etc. $\left.\right\}$, and

$$b_{11} = 3\left\{(\mu_1 + \tfrac{1}{3}\mu_{t1}) - (\mu_1 + \tfrac{1}{2}\mu_{t1})^2\right\}$$

$$b_{22} = 3\left\{(\mu_2 + \tfrac{1}{3}\mu_{t2}) - (\mu_1 + \tfrac{1}{2}\mu_{t2})^2\right\}$$

$$b_{12} = -(\mu_1 + \tfrac{1}{2}\mu_{t1})(\mu_2 + \tfrac{1}{2}\mu_{t2})$$

$$b_{i+2,i+2} = 3\left\{\bar{\mu}_1(\bar{\mu}_2 + \bar{\mu}_3) + \frac{\bar{\mu}_1\bar{\mu}_2 l_2}{l_1}\right\}$$

$$b_{i+n_1+2,i+n_1+2} = 3\left\{\bar{\mu}_1\bar{\mu}_2\frac{l_1}{l_2} + \bar{\mu}_2(\bar{\mu}_1 + \bar{\mu}_3)\right\}$$

and $$[K] = m\omega^2 [B] \qquad (3.4.6)$$

where [B] is a square matrix of size n_1+n_2+2

$$[B] = \begin{bmatrix} b_{11} & b_{12} & -- & 0 & -- & 0 \\ & b_{22} & -- & 0 & -- & 0 \\ & & . & & & \\ \text{Sym.} & & & . & & \\ & & & & & . \end{bmatrix}$$

3.5 EQUATIONS OF MOTION

Using Lagrange's equations:

$$\frac{d}{dt}\left[\frac{\partial L}{\partial \dot{q}_j}\right] - \frac{\partial L}{\partial q_j} = Q_j \quad ; \quad j = 1.2., \ldots N \qquad (3.5.1)$$

where,

q_j : generalized coordinates

L : Lagrangian = T - U = K.E. - P.E.

Q_j : generalized force (not arising from potential, non-conservative)

For our problem, $Q_j = 0$

$$q_j = \left\{ \hat{y}_1,\ \hat{y}_2,\ q_{11},\ q_{21} \cdots q_{n_1 1},\ q_{12},\ q_{22} \cdots q_{n_2 2} \right\}^T \tag{3.5.2}$$

Denoting $\hat{y}_1 = q_1$; $\hat{y}_2 = q_2$

and, $q_{1i} = q_{i+2}$; $i = 1,2 \ldots n_1$

also, $q_{2i} = q_{i+n_1+2}$; $i = 1,2 \ldots n_2$

We can write expressions for K.E. and P.E. (obtained earlier) as,

$$T = \frac{1}{2} \{\dot{q}_j\}^T [M] \{\dot{q}_j\} \tag{3.5.3}$$

and $$V = \frac{1}{2} \{q_j\}^T [K] \{q_j\} \tag{3.5.4}$$

where [M] and [K] are given by (3.3.4) and (3.4.6) respectively. then Eq. (3.5.1) becomes simply,

$$[M] \{\ddot{q}\} + [K] \{q\} = \{0\} \tag{3.5.5}$$

which is a standard eigenvalue problem.

Premultiplying by $[M]^{-1}$ and putting $[D] = [M]^{-1} [K]$, we have

$$\{\ddot{q}\} + [D] \{q\} = \{0\} \tag{3.5.6}$$

The eigenvalues of [D] are simply the squares of the frequencies of vibration whereas the eigenvectors describe the modeshapes.

3.6 RESULTS AND DISCUSSIONS

Numerical results were obtained for the following system configuration.

Masses : $m_1 = 10^5$ kg

: $m_2 = 10^4$ kg

: $m_3 = 5 \times 10^3$ kg

Tether lengths and masses : $l_1 + l_2 = 10$ km

: $m_{t1} = 10$ kg

: $m_{t2} = 50$ kg

Initial perigee height : $R_p = 500$ km

For the above values, the mass matrix [M] and the stiffness matrix [K] were obtained and the corresponding eigen problem, Eq. (3.5.6), was solved for two elements each for the upper and lower tethers. Thus, six natural frequencies and corresponding eigen vectors were obtained. The Figs. 3.4 to 3.10 plot the mode shapes for these eigen vectors. In the lowest frequency modes, we can see an almost straight tether although the masses have been displaced from their original vertical configuration. Since the lowest modes dominate in determining the actual shape of a vibrating continuous infinite degree of freedom system, we can conclude that tether displacements due to transverse vibrations are negligible. A few figures also show the plot for higher frequency modes. Here, we can see continuous deformtion of the tethers. The noticeable feature, here is that the deformations in upper and lower tethers are virtually independent of each other.

Tables 3.1 to 3.6 list the first few modal frequencies for various combinations of mass ratios. The frequencies appear to be quite independent of variations in the tether masses, m_{t1} and m_{t2}

for all practical purposes when a reasonably light tether is assumed. The orbital frequency which depends upon the semi-major axis of the orbit undergoes relatively minor variations. It is interesting to note that the lowest mode frequency is of the same order as that of the orbital frequency.

CHAPTER IV

CONCLUDING REMARKS

4.1 CLOSING REMARKS

Some important features associated with the two dynamic problems involving tethered space transportation systems considered here are summarized below:

4.1.1 Payload Resease

The first part looks into the effects of the eccentricity on the payload raising potential of the tether used for its deployment from the space shuttle placed in an elliptic orbit. The influence of pitching librations has also been taken into account while the roll has been ignored. Unlike the "forward swing zero libration", approach of Conway[15] that requires trial and error to determine the optimal tether cut-off location, a rather direct method of maximizing the total subsatellite energy has been employed here. The study clearly demonstrates the usefulness of placing the dumb-bell tethered space shuttle system in a highly elliptic orbit as it enables a substantially enhanced tether payload raising capability. In some extreme cases, e.g., for an orbital eccentricity of 0.5, the increase in the subsatellite major axis can go upto as high as ~ 50 times the tether-length.

With some additional pitching disturbances incidental to tether deployment or miscellaneous space operations, this figure of merit is likely to be even higher. This finding may add further to the multitude of spin-offs of the tether concept already on the anvil.

4.1.2 Tether Vibrations

Here, the in-plane transverse vibrations of the two tethers connecting a three-body constellation in a near-Earth circular orbit have been investigated. Attention is focussed only on the frequencies of vibrations in the lone useful equilibrium configuration aligned with the local vertical. The natural frequencies of the first few important modes are obtained using finite element approach. The frequencies turn out to be quite independent of the tether mass particularly when the tether is a relatively light. It is interesting to note that deformation of the upper and the lower tether remain virtually unaffected by each other.

4.2 SUGGESTIONS FOR FURTHER WORK

(1) The study of payload release can be extended by taking the deployment of tether into consideration as well as all the environment forces into account, such as aerodynamic drag, oblateness of the Earth etc. It may also be desirable to treat the problem in utmost generality when vibrations and the librations both are considered.

(2) The optimal location in the payload release is searched only during the first revolution around the Earth. It is feasible to further augment the orbit size gains by extending this search to a few more revolutions of the tethered space system. This may

however, imply a longer waiting time before the "optimal tether cut-off".

(3) For three body systems, longitudinal vibrations can be combined with the transverse vibrations studied presently. The resulting equilibrium configuration and stability analysis may be useful in the preliminary design of system controllers. The dynamic analysis of the system in elliptic orbits appears to be yet another logical extension of the present work.

REFERENCES

1. Tsiolkovski, K.E., "Grezi O Zanle i nebe (i) Na Vesta" (Speculations between Earth and Sky, and on Vesta; Science Fiction Works), AN SSSR, p. 35, izd-VD, Moscow,1959.

2. Lang, D.L. and Nolting, R.K., "Operation with Tethered Space Vehicles", NASA SP-138, Gemini Summary Conference,February 1967.

3. Sisson, J.M., "Development Status of First Tethered Satellite System", MCFC Report, MP-83-034, January, 1986.

4. Bonifazi, C., "Tethered Satellite Systems Core Science Equipment", AAS 86-214, Vol. 62, Proceedings of the Advances in Astronautical Sciences, Ed. P.M. Barlum, 1987.

5. Penzo, Paul A., "A Low Earth Orbit Skyhook Tether Transportation System", AAS/AIAA, Astrodynamics Specialist conference, August 1987.

6. Misra, A.K. and Modi, V.J., "Deployment and retrieval of Shuttle Supported Tethered Satellite", Journal of Guidance, Control and Dynamics, Vol. 5, No. 3, 1982, pp. 278-285.

7. Misra, A.K. and Modi, V.J., "A Survey on the Dynamics and Control of Tethered Satellite Systems", NASA/AIAA/PSN International conference on Tethers in Space, Arlington, Va., September 1986.

8. Von Tiesenhausen, G., "Future Applications of Tethers in Space", AIAA 24th Aerospace Sciences Meeting, Reno, Nevada, January 1986, Paper No. 86-0053.

9. Bekey, I., "Tethers Open New Space Options", Astronautics and Aeronautics, Vol. 21, No. 4, 1983, pp. 32-40.

10. Amier, Z.E., "On Some Transportation Problems involving tethered Satellite Systems", M.E. Thesis, Department of Mechanical Engineering, McGill University, Canada.

11. Liu, F.C., "On Dynamical formulations of a Tethered Satellite System with Mass Transfer", AIAA 23rd Aerospace Sciences Meeting, Reno, Nevada, January 1985, Paper No. 85-0117.

12. Lorenzini, E., Arnold, D.A. Grossi, M.D., and gullahorn, G.E., "Analytical Investigation of the Dynamics of Tethered Constellations in Earth Orbit", Quarterly report No. 1, Contrast NAS 8-36606, Smithsonian Institution, Astrophysical Observatory, Cambridge, Massachusetts, July 1985.

13. Modi, V.J. and Misra, A.K., "Orbital Perturbations of Tethered Satellite Systems", The Journal of Astronautical Sciences, Vol. 25, No. 3, 1977, pp. 271-278.

14. Marshall, H.K., Modern Spacecraft Dynamics and Control, John Wiley & Sons, New York, 1976.

15. Conway, Bruce, A., Kyroudis, George, A. "Advantages of Tether Release of Satellites from Elliptic Orbit", Journal of Guidance and Control, Vol. 11, No. 5, September - October, 1988.

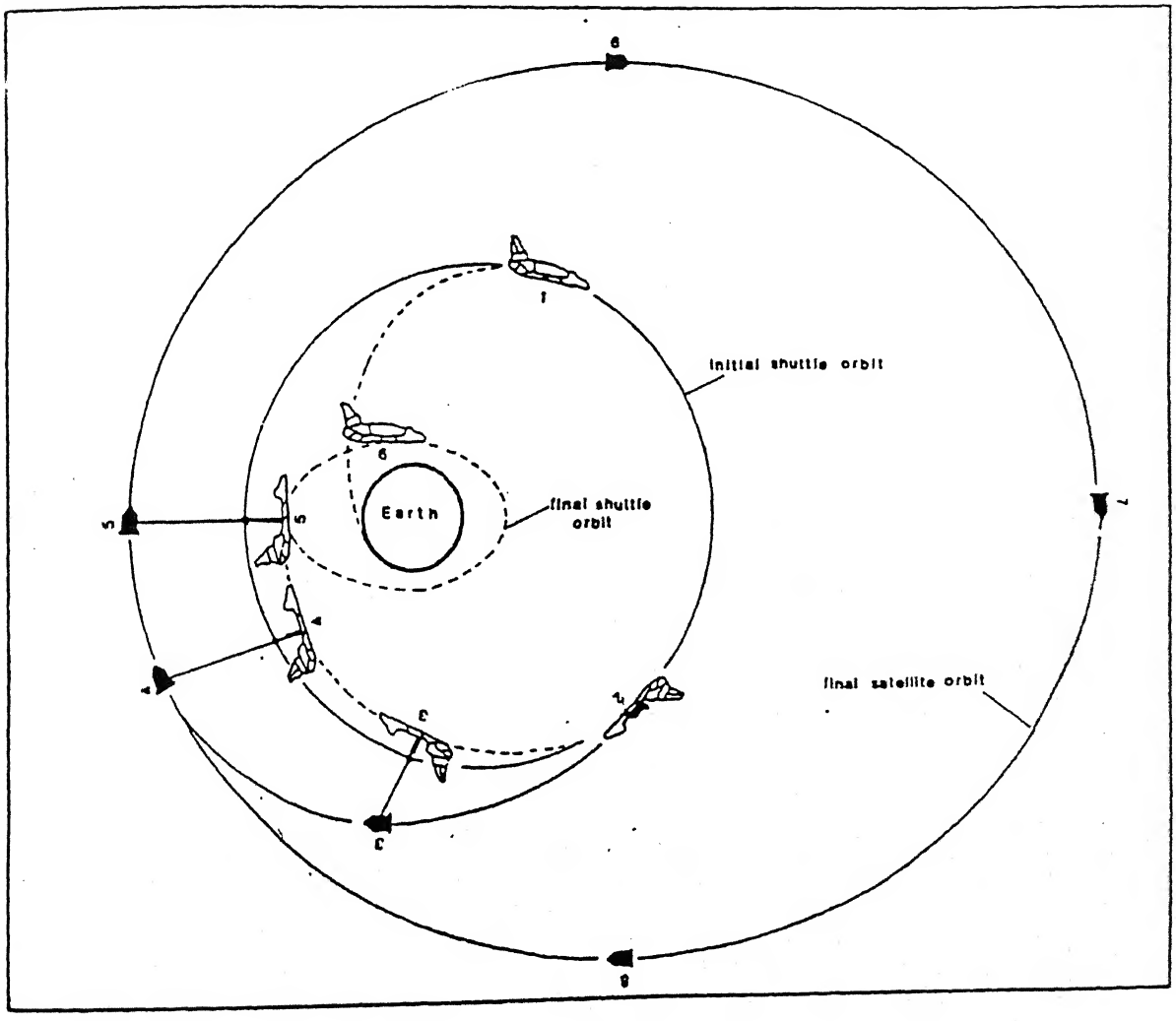

Figure 1. Concept of release of payload

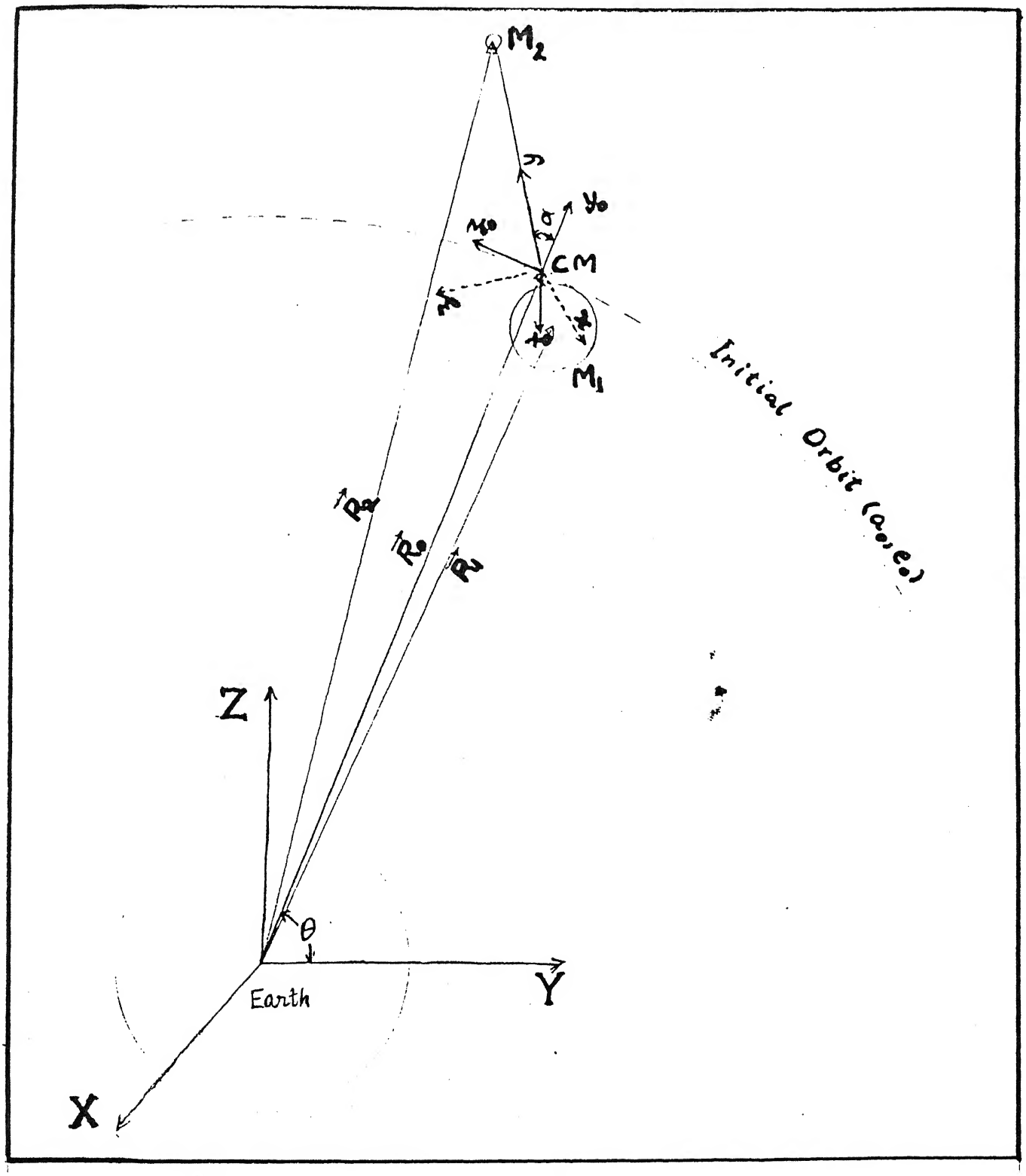

FIG. 2 : TWO BODY TETHERED SYSTEM IN SPACE

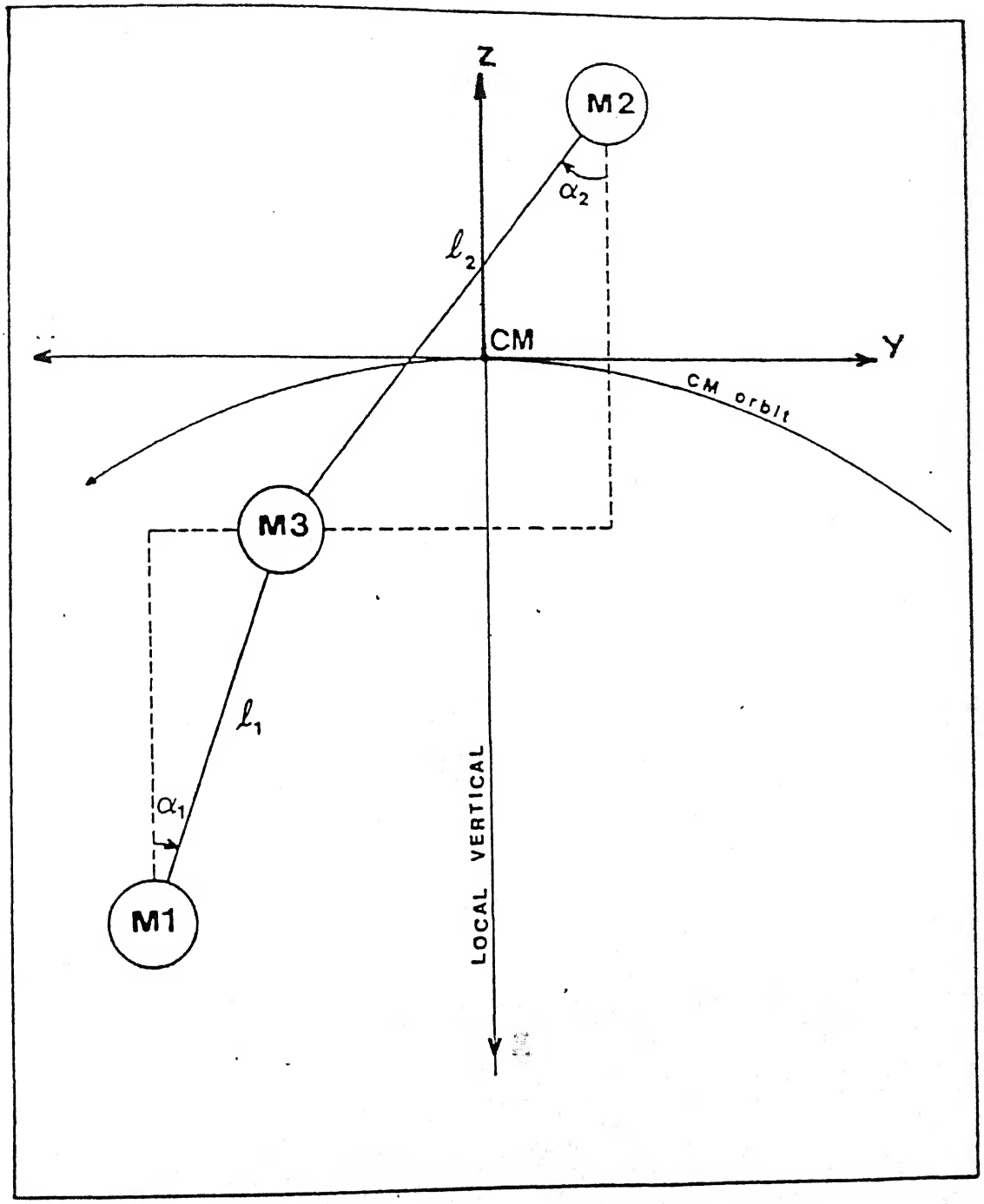

Figure 3.1 Geometry of motion of three-body tethered system.

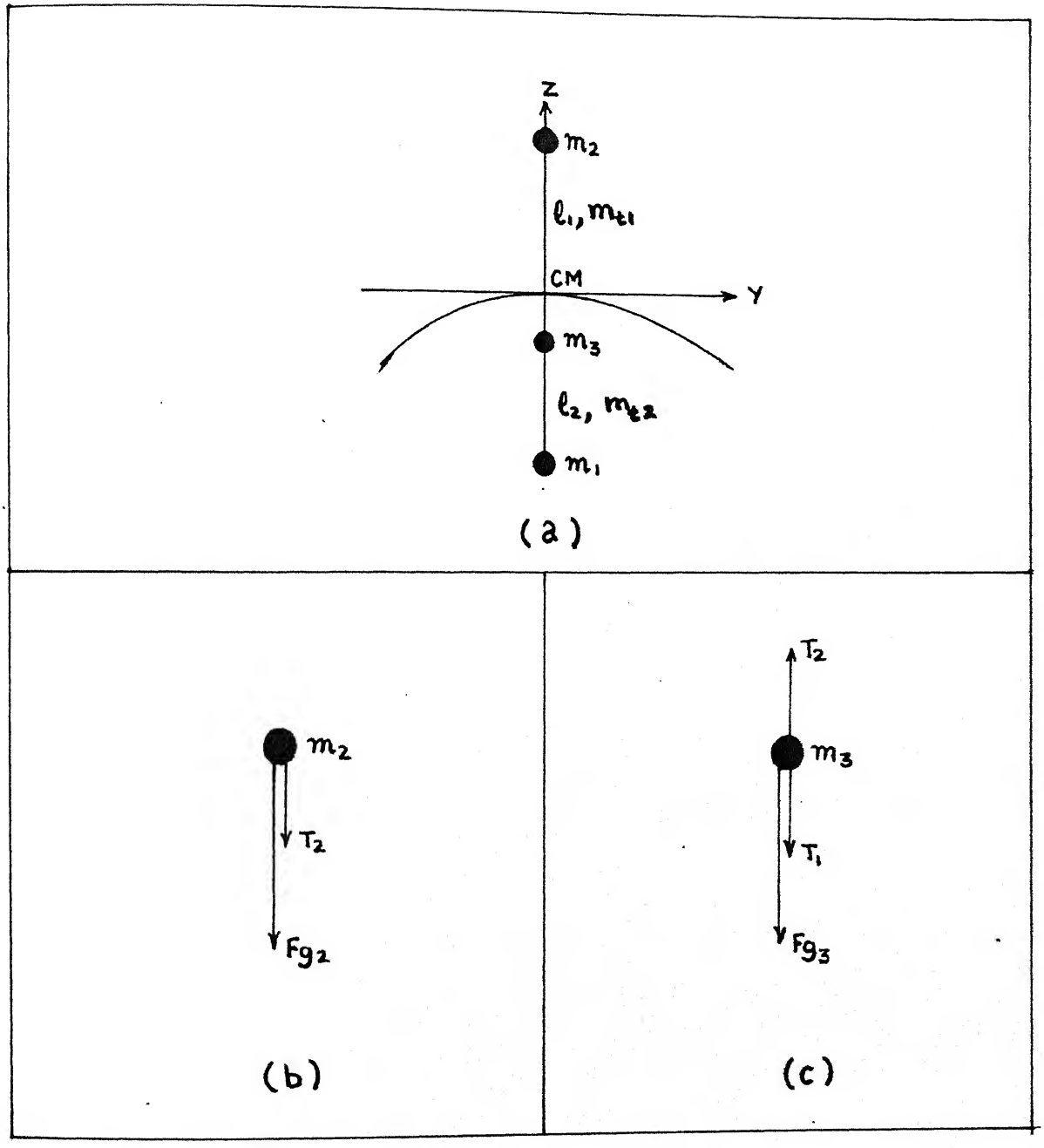

FIG. 3.2 : EQUILIBRIUM CONFIGURATION OF THREE BODY SYSTEM

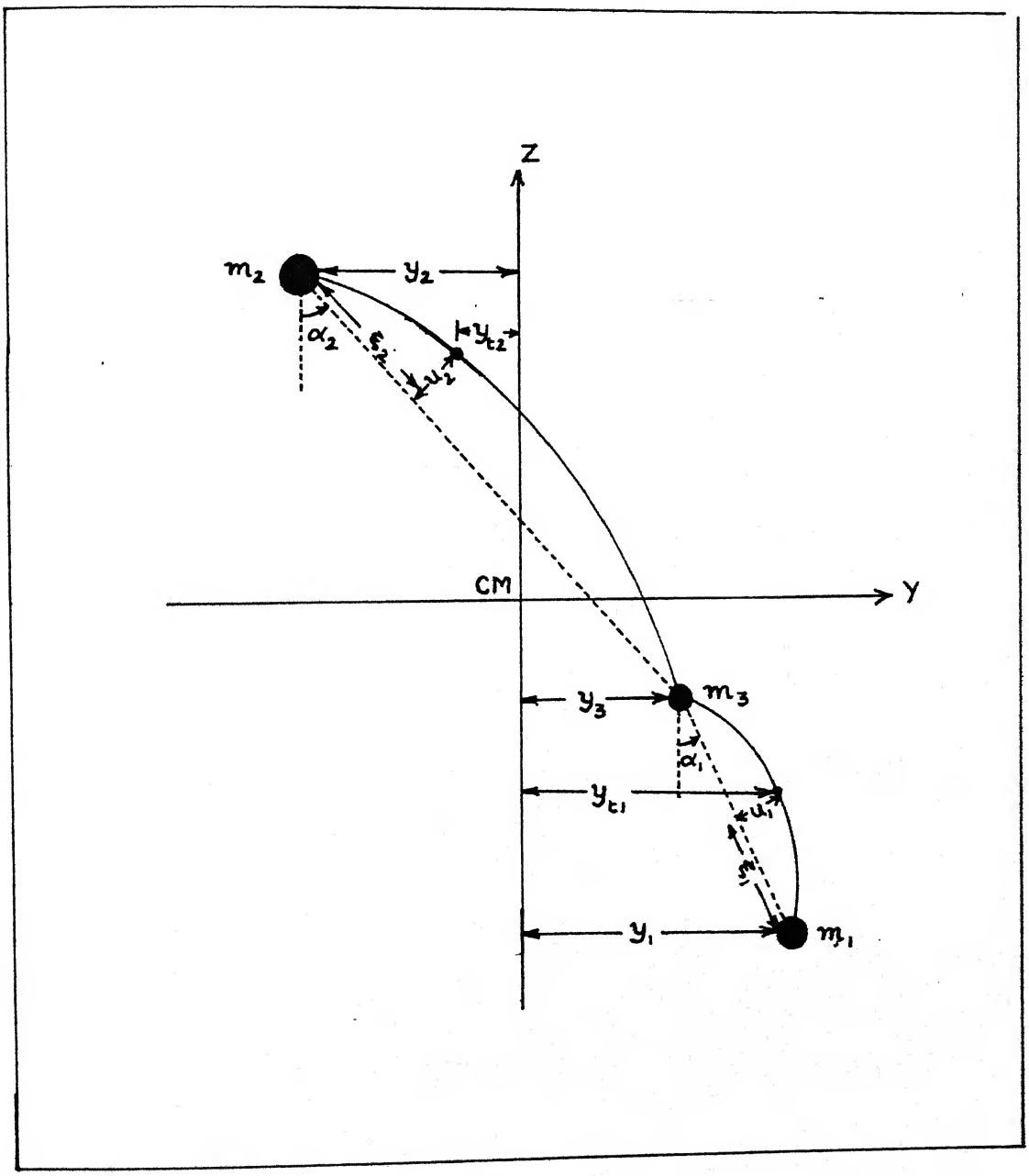

FIG. 3.3 : VIBRATION EXCITED SHAPE OF THREE BODY SYSTEM

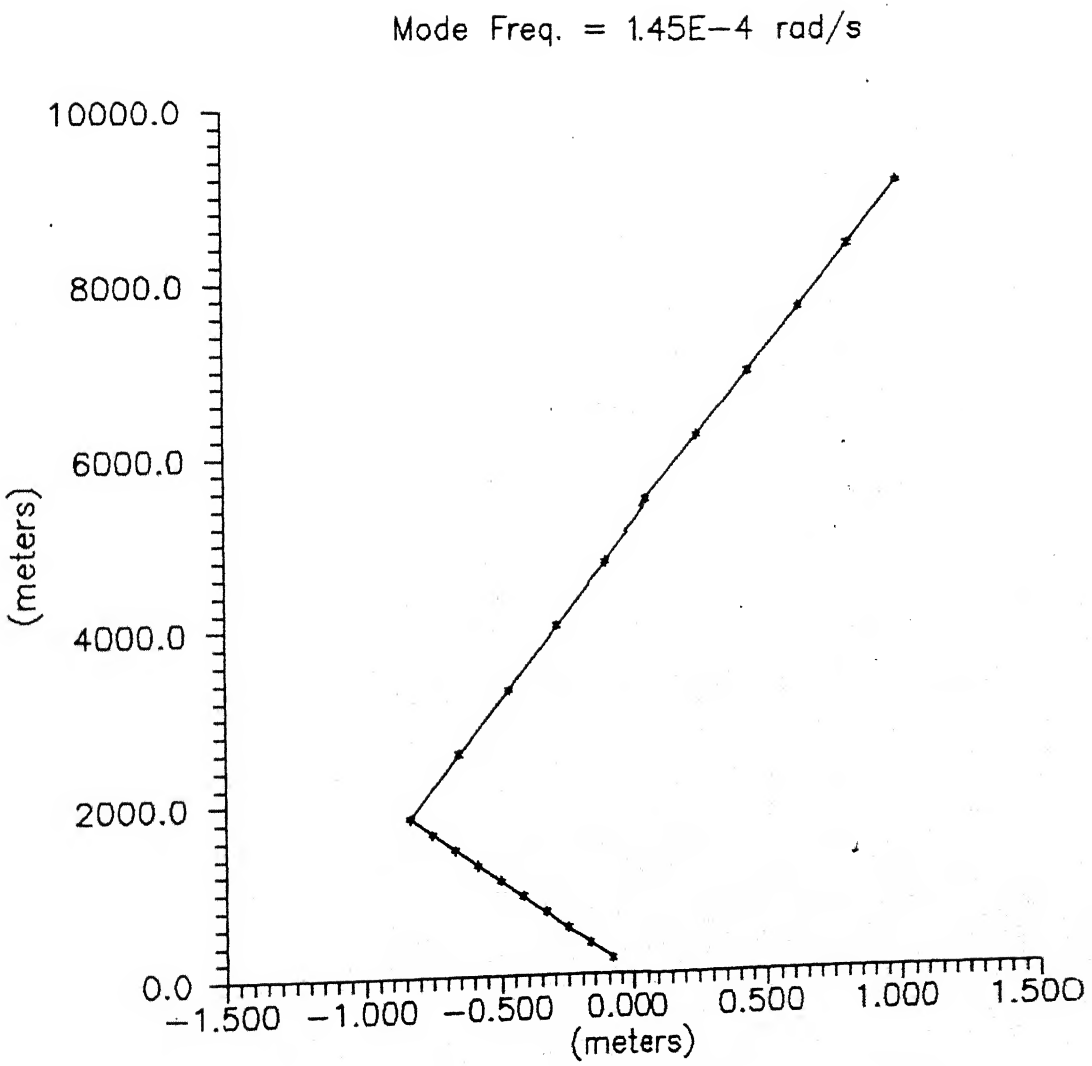

Figure 3.4 : Mode Shape for Three−body System

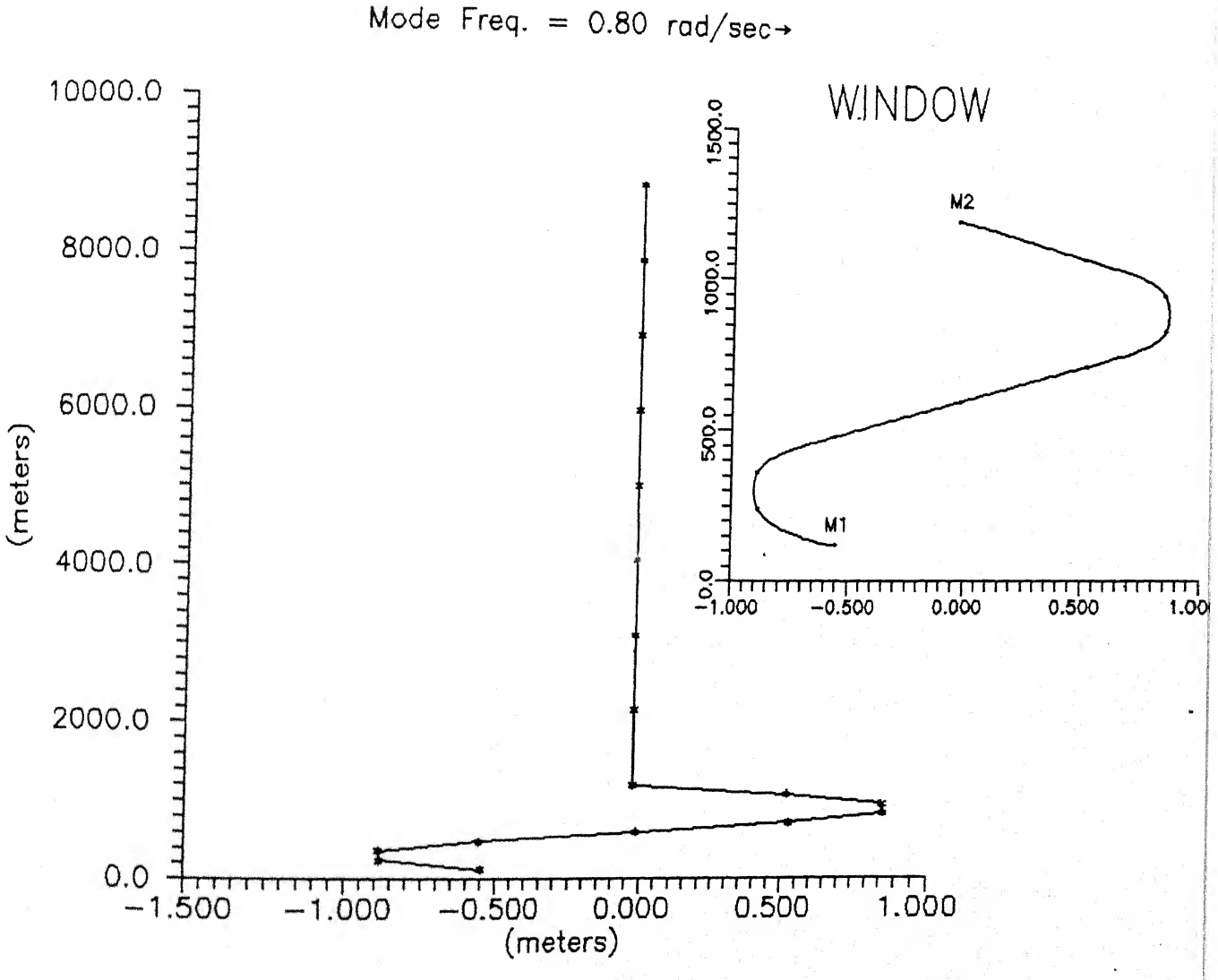

Figure 3.5 : Mode Shape for Three-body System

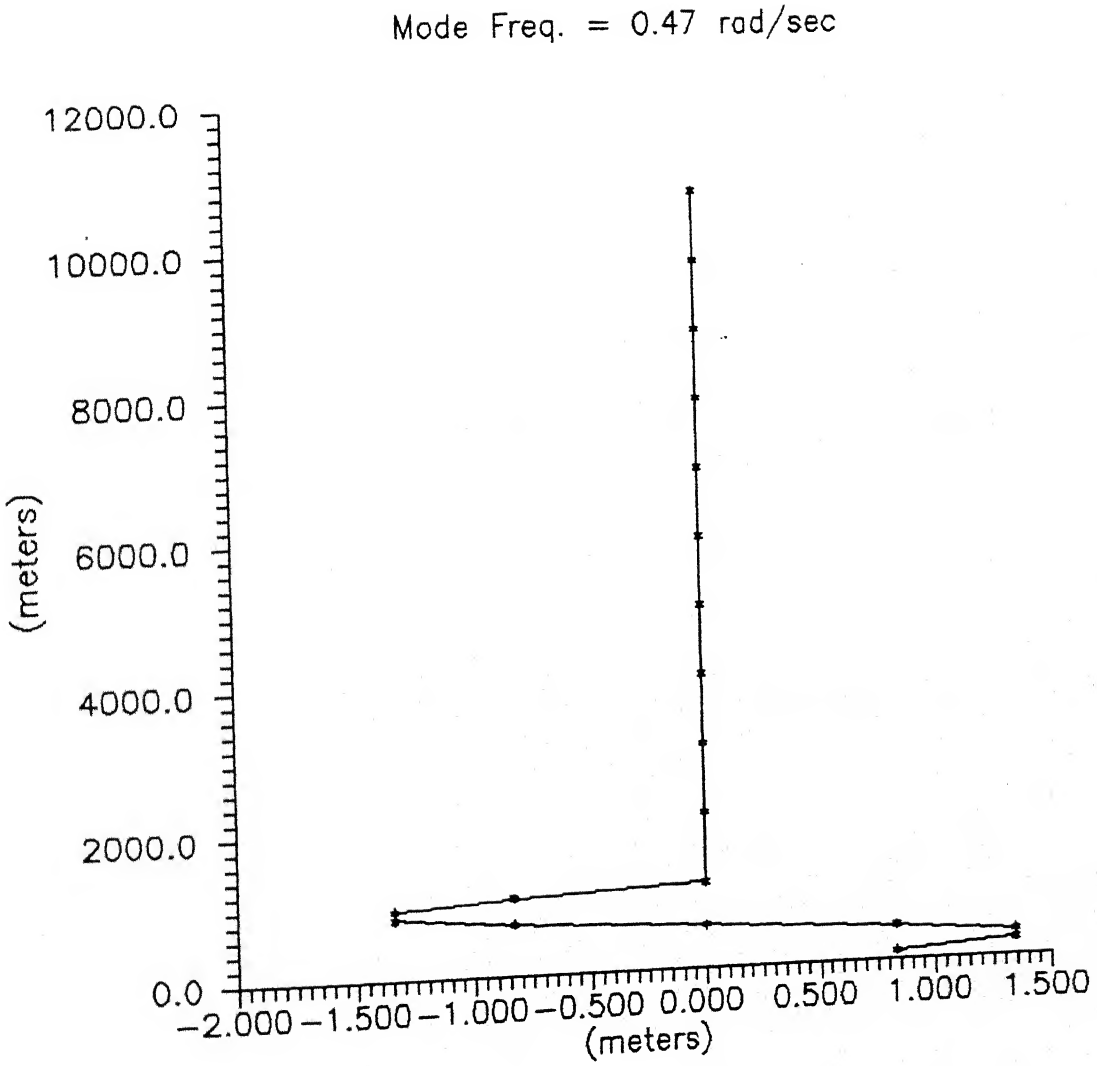

Figure 3.6 : Mode Shape for Three-body System

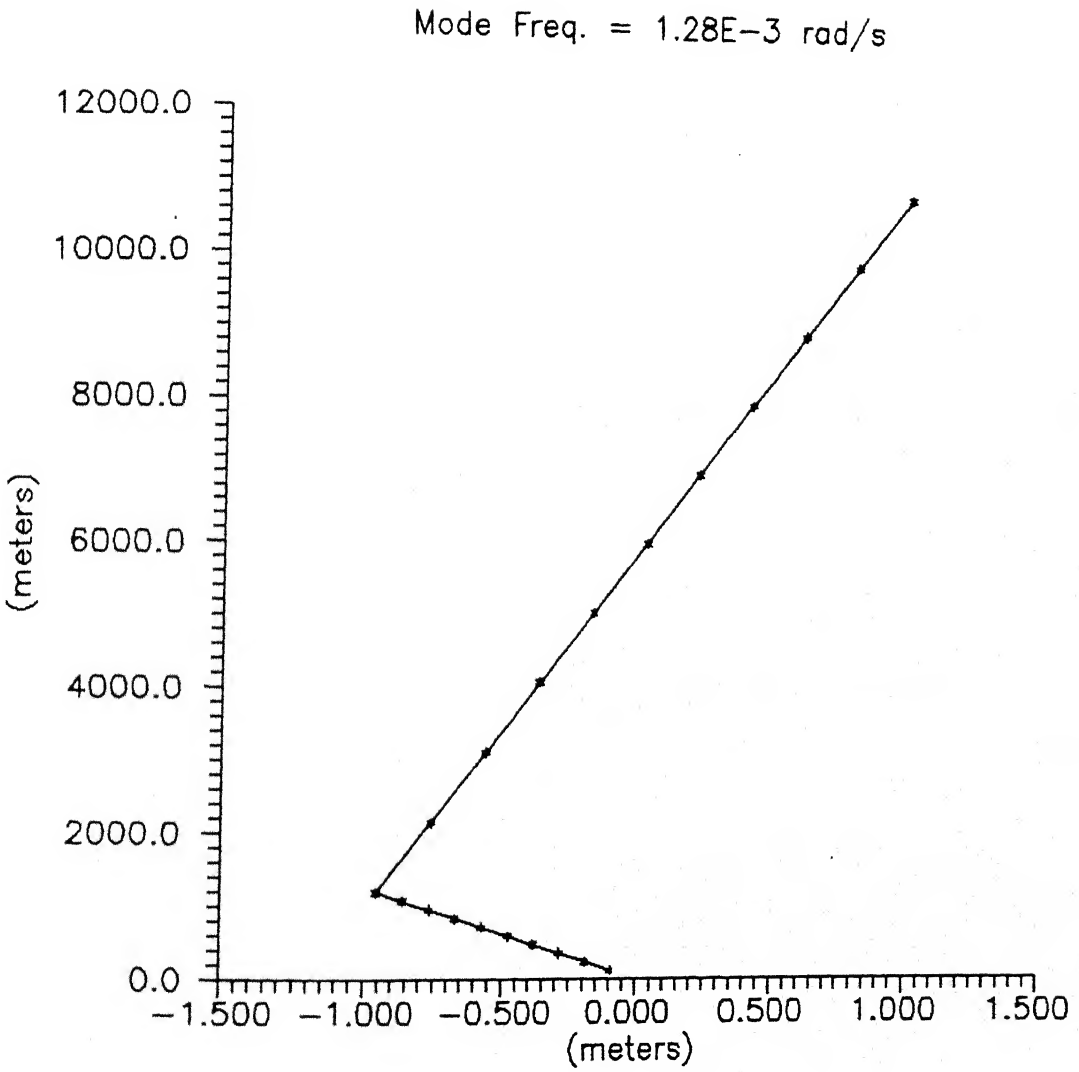

Figure 3.7 : Mode Shape for Three-body System

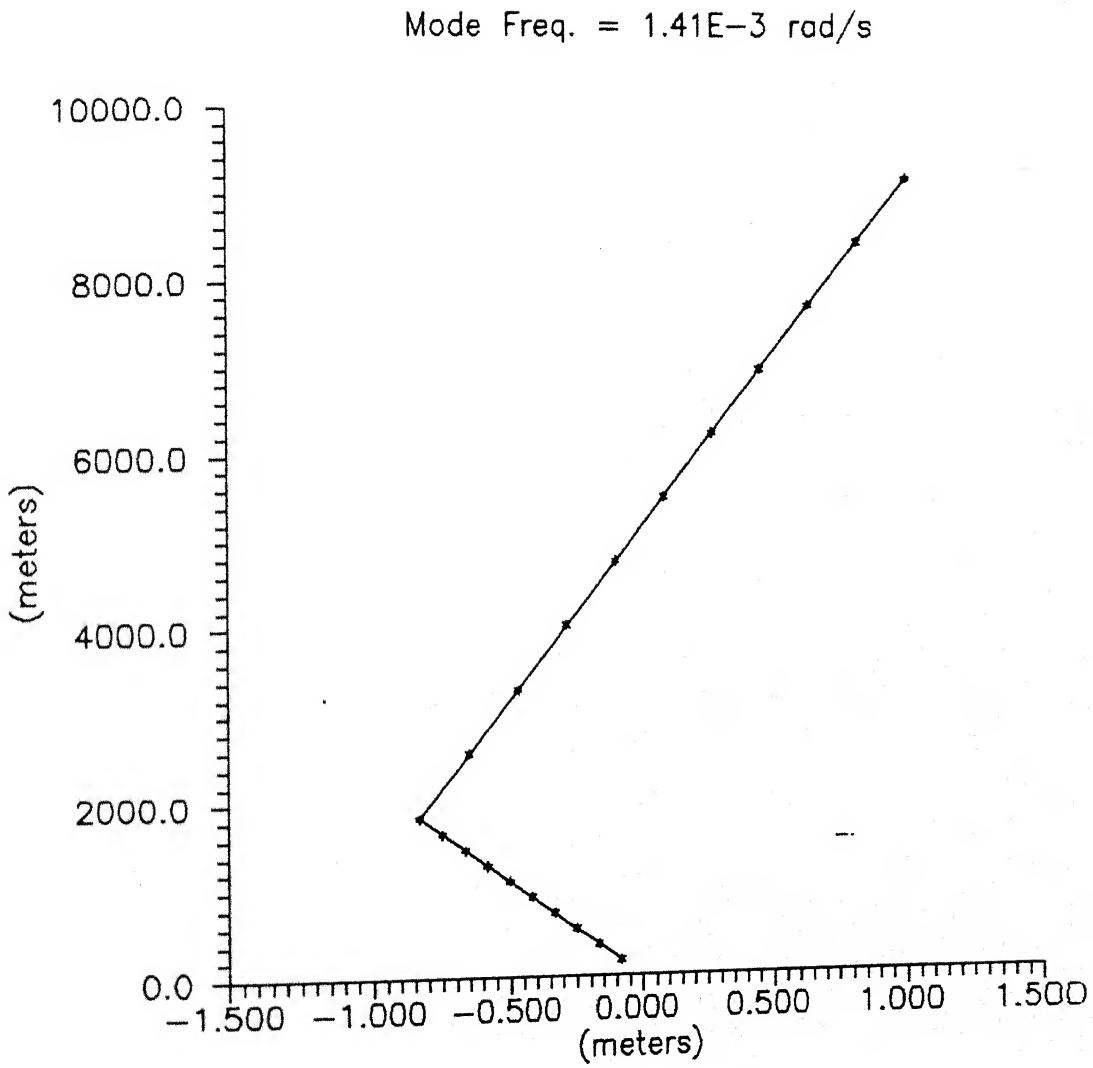

Figure 3.8 : Mode Shape for Three−body System

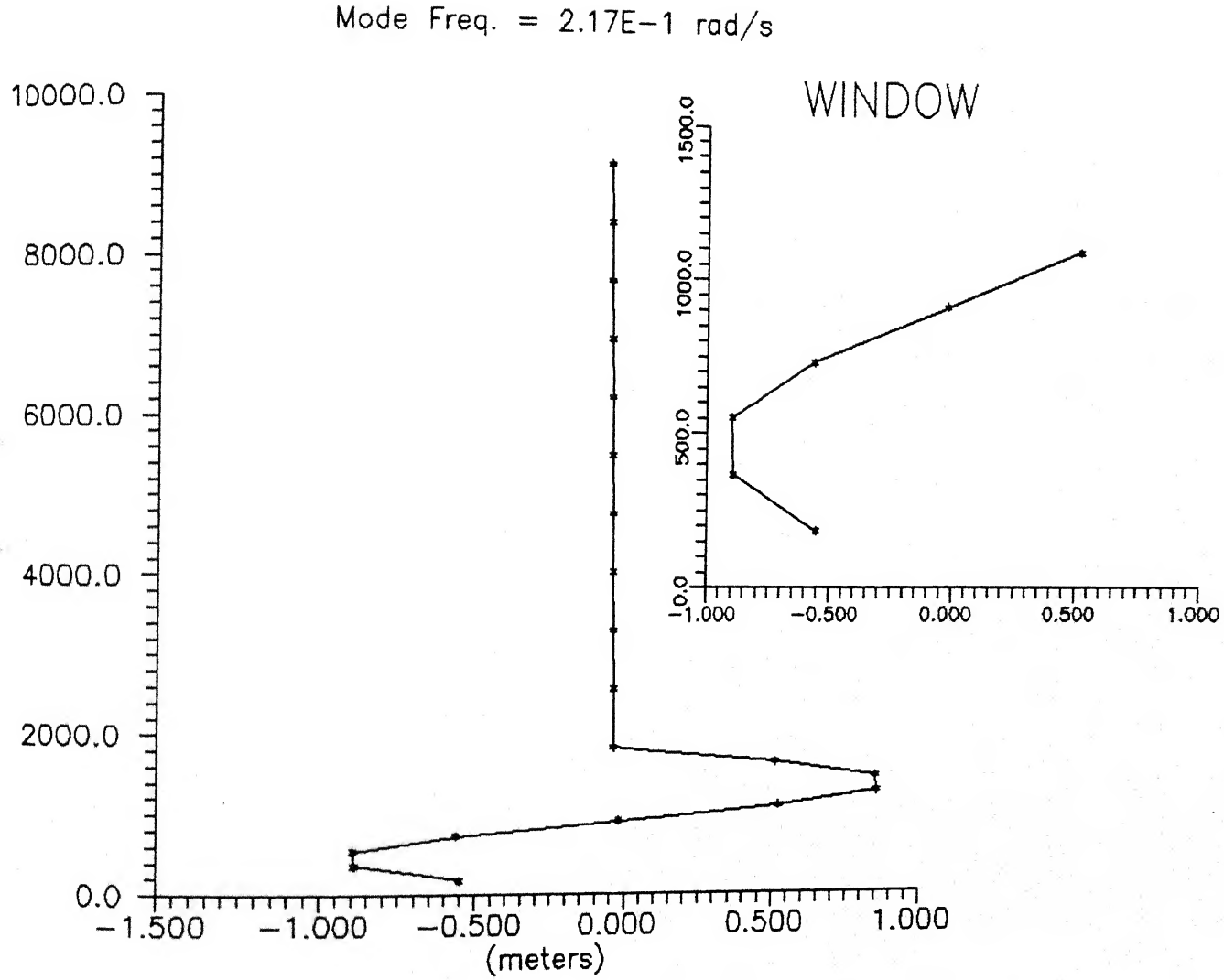

Figure 3.9 : Mode Shape for Three-body System

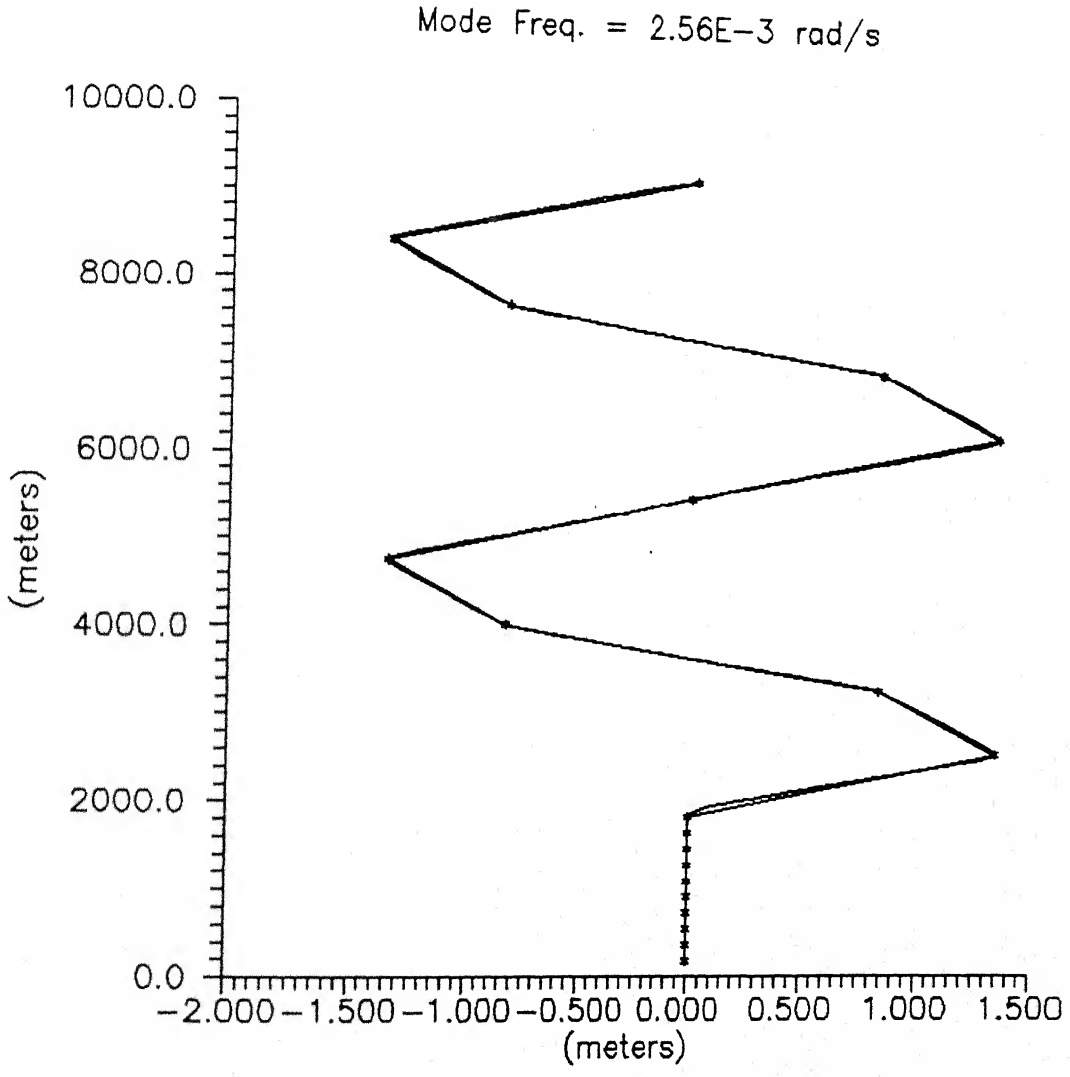

Figure 3.10: Mode Shape for Three-body System

Table 2.1

Optimum Apogee Height and Position of the System

Typical Plot : e = 0.5, $\alpha_o = 10^o$, $\alpha_o' = 0$

	Sl.No.	θ_r (deg.)	Δa_r (km.)	H_m (km.)
TOL = 1 x 10^{-4}	1	16.19	2347.14	18223.33
	2	136.48	1199.99	15149.67
	3	170.51	839.66	13835.23
	4	198.89	900.57	14099.89
	5	240.94	1488.20	15974.31
TOL = 1 x 10^{-5}	1	16.19	2347.14	18223.34
	2	136.48	1200.00	15149.85
	3	170.51	839.73	14099.31

Table 2.2

Optimum Apogee Height and Position of the System

$e = 0.0, \alpha_o = 0$

α_o'	0	0.05	0.1	0.2	0.5
θ_r (deg.)	0	118.54	95.44	72.20	40.04
Δa (km.)	420.00	535.30	536.23	539.42	565.70
H_m (km.)	740.74	985.64	987.40	994.37	1043.01

Table 2.3

Optimum Apogee Height and Position of the System

$e = 0.0, \alpha_o' = 0$

α_o (deg.)	5.8	18	45	60
θ_r (deg.)	77.80	42.41	19.70	13.40
Δa (km.)	531.30	499.94	339.52	222.95
H_m (km.)	978.10	917.9	617.8	401.02

Table 2.4

Optimum Apogee Height and Position of the System

$e = 0.01$, $\alpha_o' = 0$

α_o (deg.)	0	5.8	18	45	60
θ_r (deg.)	194.48	76.05	131.06	269.72	238.80
Δa (km.)	521.90	534.50	508.50	353.70	229.30
H_m (km.)	964.30	1068.70	1053.00	764.00	545.00

Table 2.5

Optimum Apogee Height and Position of the System

$e = 0.01$, $\alpha_o = 0$ deg.

α_o'	0.01	0.05	0.1	0.30
θ_r (deg.)	157.6	114.12	92.69	56.81
Δa (km.)	522.80	530.05	535.85	554.04
H_m (km.)	963.4	1014.4	1051.24	1126.70

Table 2.6

Optimum Apogee Height and Position of the System

$e = 0.05$, $\alpha_o = 0$ deg.

α_o'	0.02	0.1	0.3
θ_r (deg.)	115.43	81.65	50.61
Δa (km.)	507.60	546.26	593.30
H_m (km.)	1588.05	1630.93	1733.77

Table 2.7

Optimum Apogee Height and Position of the System

$e = 0.05$

α_o (deg.)	5.8	45	120
α_o'	0.01	0.01	0.3
θ_r (deg.)	67.22	294.44	357.88
Δa (km.)	557.38	438.32	273.10
H_m (km.)	1609.80	1451.26	1215.15

Table 2.8

Optimum Apogee Height and Position of the System

$e = 0.1$, $\alpha_o = 0$ (deg.)

α_o'	0.02	0.1	0.3
θ_r (deg.)	0.00	342.05	41.70
Δa (km.)	556.70	720.90	660.80
H_m (km.)	2529.29	2865.90	2673.54

Table 2.9

Optimum Apogee Height and Position of the System

$e = 0.1$

α_o (deg.)	5.8	45	90	120
α_o'	0.00	0.01	0.05	0.1
θ_r (deg.)	300.00	17.00	274.45	343.87
Δa (km.)	699.28	430.31	71.72	330.50
H_m (km.)	2723.42	2296.14	1609.00	2125.50

Table 2.10

Optimum Apogee Height and Position of the System

e = 0.5

α_o (deg.)	0	0	10	45	90
α_o'	0.01	0.1	0.00	0.001	0.1
θ_r (deg.)	0.00	0.00	16.90	10.65	247.40
Δa (km.)	2336.22	2486.97	2347.14	1644.73	163.00
H_m (km.)	18209.00	18510.70	18223.30	16850.95	13916.00

Table 3.1

Natural Frequencies for the Variation of Mass m_1.

μ_1	μ_2	μ_3	μ_{t1}	Ω rad/s	Last Freq. rad/s	First Freq. rad/s
9.69×10^{-7}	8.91×10^{-1}	9.69×10^{-2}	6.78×10^{-4}	9.96×10^{-4}	4.93×10^{-3}	2.05×10^{-4}
4.66×10^{-6}	8.32×10^{-1}	9.33×10^{-2}	6.53×10^{-4}	9.96×10^{-4}	4.98×10^{-3}	3.27×10^{-4}
8.91×10^{-5}	8.91×10^{-1}	8.91×10^{-2}	6.24×10^{-4}	9.96×10^{-4}	4.88×10^{-3}	8.08×10^{-4}
3.28×10^{-4}	8.97×10^{-1}	9.87×10^{-2}	6.60×10^{-4}	9.96×10^{-4}	9.06×10^{-3}	1.00×10^{-3}
4.94×10^{-3}	8.94×10^{-1}	9.94×10^{-2}	6.46×10^{-4}	9.96×10^{-4}	2.77×10^{-2}	1.58×10^{-3}
1.07×10^{-2}	8.97×10^{-1}	8.97×10^{-2}	6.35×10^{-4}	9.96×10^{-4}	1.31×10^{-2}	1.58×10^{-3}
1.00×10^{-2}	8.10×10^{-1}	8.99×10^{-2}	6.93×10^{-5}	9.96×10^{-4}	7.40×10^{-1}	1.59×10^{-3}

Table 3.2

Natural Frequencies for the Variation of Mass m_2.

μ_1	μ_2	μ_3	μ_{t1}	Ω rad/s	Last Freq. rad/s	First Freq. rad/s
$8.91x10^{-1}$	$9.68x10^{-7}$	$9.69x10^{-2}$	$6.78x10^{-4}$	$9.96x10^{-4}$	$1.97x10^{-2}$	$1.66x10^{-5}$
$8.33x10^{-1}$	$4.66x10^{-6}$	$9.33x10^{-2}$	$6.53x10^{-4}$	$9.96x10^{-4}$	$2.04x10^{-2}$	$1.43x10^{-5}$
$8.91x10^{-1}$	$8.91x10^{-5}$	$8.91x10^{-2}$	$6.24x10^{-4}$	$9.96x10^{-4}$	$2.02x10^{-2}$	$1.27x10^{-4}$
$8.97x10^{-1}$	$3.28x10^{-4}$	$9.87x10^{-2}$	$6.60x10^{-4}$	$9.96x10^{-4}$	$2.03x10^{-2}$	$5.54x10^{-4}$
$8.94x10^{-1}$	$4.94x10^{-3}$	$9.94x10^{-2}$	$6.46x10^{-4}$	$9.96x10^{-4}$	$3.40x10^{-2}$	$1.62x10^{-3}$
$8.97x10^{-1}$	$1.07x10^{-2}$	$8.97x10^{-3}$	$6.35x10^{-4}$	$9.96x10^{-4}$	$8.43x10^{-2}$	$6.49x10^{-4}$
$8.10x10^{-1}$	$1.00x10^{-2}$	$8.98x10^{-2}$	$6.92x10^{-5}$	$9.96x10^{-4}$	$7.42x10^{-1}$	$6.00x10^{-4}$

Table 3.3

Natural Frequencies for the Variation of Mass m_3.

μ_1	μ_2	μ_3	μ_{t1}	Ω rad/s	Last Freq. rad/s	First Freq. rad/s
8.91×10^{-1}	9.69×10^{-2}	9.69×10^{-7}	6.78×10^{-4}	9.96×10^{-4}	8.23×10^{-2}	1.41×10^{-3}
8.32×10^{-1}	9.32×10^{-2}	4.66×10^{-6}	6.53×10^{-4}	9.96×10^{-4}	2.16×10^{-1}	1.36×10^{-3}
8.91×10^{-1}	8.91×10^{-2}	8.91×10^{-5}	6.24×10^{-4}	9.96×10^{-4}	1.10×10^{-1}	1.40×10^{-3}
8.97×10^{-1}	9.87×10^{-2}	3.28×10^{-4}	6.60×10^{-4}	9.96×10^{-4}	4.98×10^{-2}	1.41×10^{-3}
8.94×10^{-1}	9.94×10^{-2}	4.94×10^{-3}	6.46×10^{-4}	9.96×10^{-4}	4.23×10^{-2}	1.41×10^{-3}
8.97×10^{-1}	8.97×10^{-2}	1.07×10^{-2}	6.35×10^{-4}	9.96×10^{-4}	3.74×10^{-2}	1.42×10^{-3}
8.09×10^{-1}	8.98×10^{-2}	1.00×10^{-2}	6.92×10^{-5}	9.96×10^{-4}	2.22	1.34×10^{-3}

Table 3.4

Natural Frequencies for the Variation of Tether Mass m_{t1}.

μ_1	μ_2	μ_3	μ_{t1}	Ω rad/s	Last Freq. rad/s	First Freq. rad/s
8.69×10^{-1}	8.69×10^{-2}	4.34×10^{-2}	4.34×10^{-5}	9.96×10^{-4}	2.44×10^{-2}	1.45×10^{-3}
8.69×10^{-1}	8.69×10^{-2}	4.34×10^{-2}	8.69×10^{-5}	9.96×10^{-4}	6.60×10^{-1}	1.45×10^{-3}
8.69×10^{-1}	8.69×10^{-2}	4.34×10^{-2}	1.30×10^{-4}	9.96×10^{-4}	1.59×10^{-1}	1.45×10^{-3}
8.69×10^{-1}	8.69×10^{-2}	4.34×10^{-2}	2.17×10^{-4}	9.96×10^{-4}	8.43×10^{-2}	1.45×10^{-3}
8.69×10^{-1}	8.69×10^{-2}	4.34×10^{-2}	3.04×10^{-4}	9.96×10^{-4}	6.10×10^{-2}	1.45×10^{-3}
8.69×10^{-1}	8.69×10^{-2}	4.34×10^{-2}	4.34×10^{-4}	9.96×10^{-4}	4.56×10^{-2}	1.45×10^{-3}
8.69×10^{-1}	8.69×10^{-2}	4.34×10^{-2}	6.51×10^{-4}	9.96×10^{-4}	3.71×10^{-2}	1.45×10^{-3}
8.69×10^{-1}	8.69×10^{-2}	4.34×10^{-2}	8.68×10^{-4}	9.96×10^{-4}	4.02×10^{-2}	1.45×10^{-3}
8.69×10^{-1}	8.69×10^{-2}	4.34×10^{-2}	1.30×10^{-3}	9.96×10^{-4}	4.64×10^{-2}	1.45×10^{-3}

Table 3.5

Natural Frequencies for the Variation of Tether Mass m_{t2}.

μ_1	μ_2	μ_3	μ_{t1}	Ω rad/s	Last Freq. rad/s	First Freq. rad/s
8.69×10^{-1}	8.69×10^{-2}	4.34×10^{-2}	4.34×10^{-4}	9.96×10^{-4}	2.42×10^{-1}	1.45×10^{-3}
8.69×10^{-1}	8.69×10^{-2}	4.34×10^{-2}	4.34×10^{-4}	9.96×10^{-4}	1.26×10^{-1}	1.45×10^{-3}
8.69×10^{-1}	8.69×10^{-2}	4.34×10^{-2}	4.34×10^{-4}	9.96×10^{-4}	8.72×10^{-2}	1.45×10^{-3}
8.69×10^{-1}	8.69×10^{-2}	4.34×10^{-2}	4.34×10^{-4}	9.96×10^{-4}	4.32×10^{-2}	1.45×10^{-3}
8.69×10^{-1}	8.69×10^{-2}	4.34×10^{-2}	4.34×10^{-4}	9.96×10^{-4}	3.02×10^{-1}	1.45×10^{-3}

Table 3.6

Natural Frequencies for the Variation of Orbital Frequency Ω .

μ_1	μ_2	μ_3	μ_{t1}	Ω rad/s	Last Freq. rad/s	First Freq. rad/s
$8.69\text{x}10^{-1}$	$8.69\text{x}10^{-2}$	$4.34\text{x}10^{-2}$	$4.34\text{x}10^{-4}$	$1.06\text{x}10^{-3}$	$2.58\text{x}10^{-1}$	$1.54\text{x}10^{-3}$
$8.69\text{x}10^{-1}$	$8.69\text{x}10^{-2}$	$4.34\text{x}10^{-2}$	$4.34\text{x}10^{-4}$	$9.03\text{x}10^{-4}$	$7.90\text{x}10^{-2}$	$1.31\text{x}10^{-3}$
$8.69\text{x}10^{-1}$	$8.69\text{x}10^{-2}$	$4.34\text{x}10^{-2}$	$4.34\text{x}10^{-4}$	$4.88\text{x}10^{-4}$	$3.20\text{x}10^{-2}$	$7.08\text{x}10^{-4}$
$8.69\text{x}10^{-1}$	$8.69\text{x}10^{-2}$	$4.34\text{x}10^{-2}$	$4.34\text{x}10^{-4}$	$2.34\text{x}10^{-4}$	$1.13\text{x}10^{-2}$	$3.30\text{x}10^{-4}$

AE-1990-M-JHA-ANA